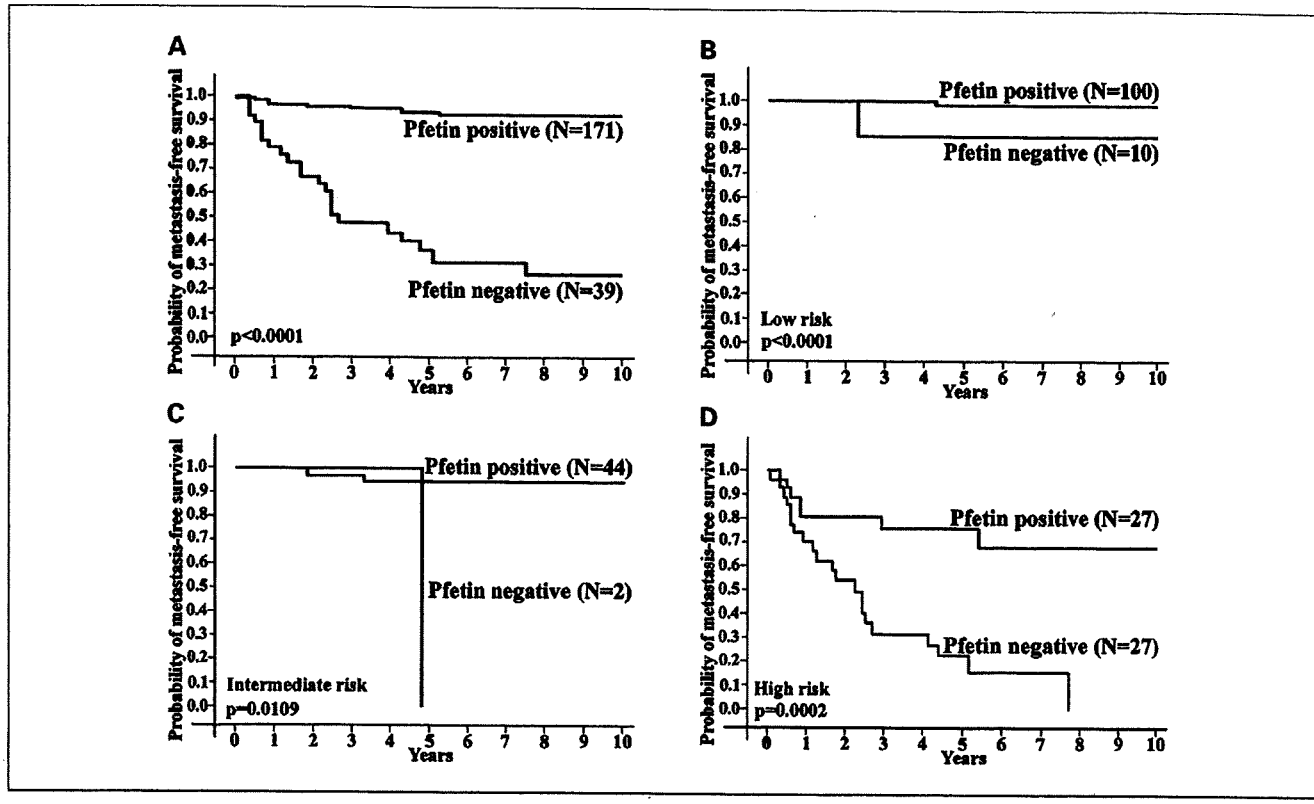

Fig. 3. Pfetin expression in the primary tumor samples was predictive of the metastasis-free survival period. Statistically significant differences in the metastasis-free survival period were observed between the pfetin-positive and pfetin-negative groups ($P < 0.0001$) both for the M0 GIST patients overall (*A*) and within each risk group of patients (*B-D*).

clearly indicate that prognosis relying solely on the established risk classification system is not sufficiently accurate to determine the post-operative therapeutic strategy for GIST patients, and the use of pfetin expression may further refine the prognostic criteria so as to identify patients who may benefit from additional therapy.

Discussion

Employing proteomics tools, we identified 43 protein variants corresponding to 25 distinct gene products that distinguished GIST patients according to their clinical outcome. The discriminating power of this set of proteins may be developed for use in a clinical setting. However, albeit useful to describe complex clinical variables, cutting-edge proteomic technologies cannot be transferred easily to a hospital setting, considering the high installation costs and labor intensity, the low throughput, and the required operational skills. A smaller number of proteins, measurable by simpler techniques, may be preferable for use in practice. With this notion, we showed that pfetin expression can be examined by SDS-PAGE/Western blotting, immunohistochemistry, and quantitative RT-PCR. Moreover, using a large-scale sample set, we showed that the expression levels of pfetin, as evaluated by immunohistochemistry, are predictive of patient outcome. Therefore, evaluation of pfetin expression can be applied in a clinical setting using the existing examination protocol and may allow the identification of a high-risk patient group that may benefit from adjuvant therapy, such as treatment with imatinib, while it may also help spare low-risk patients unnecessary treatment. As mass spectrometric global surveys for phosphorylated proteins identified pfetin as a phosphorylated protein (34, 35), the multiple protein spots of pfetin may correspond to the different phosphorylation variants.

Recently, Kang et al. (33) did a proteomic study on 12 GIST samples using two-dimensional gel electrophoresis and reported that pfetin overexpression (C13orf2 in their report) correlated with histologic grading and the presence of c-kit mutations. In contrast, our results indicated that pfetin expression is inversely correlated with histologic grading (Figs. 1 and 2), and that pfetin expression levels are not associated with c-kit mutation status (Supplementary Tables S1 and S3). Moreover, the proteins reported to correlate with histologic malignancy by Kang et al. (33), including Annexin V, HMGB1, glutamate dehydrogenase 1, and fibrinogen β chain RoXaN (33), were not identified as such in our study, whereas 24 gene products identified in this study were not listed in their report (33). As these discrepancies may be due to differences in patient populations and proteomic modalities used, an international project to integrate all reported proteomic data in a common proteomic platform is needed to elucidate the molecular background of GISTs.

Although pfetin is known to contain a voltage-gated potassium (K^+) channel tetramerization domain (25), its function in the process of cancer development and progression

is unknown. Although GISTs originate from Cajal cells, immunohistochemistry revealed that pfetin was absent in Gajal cells (Supplementary Fig. S5). Proteomic analysis of pfetin-associated proteins may provide clues to understanding the role of pfetin in GIST development and progression.

Our study has the limitation of not detecting proteins expressed in low levels. We did not observe overexpression of the kit (36–41) or PDGFRA gene products, or loss of CD44 (42) or p16 (11, 12). In addition, we did not detect CD34 (18) or connexin 43 (43) expression, reported to be commonly up-regulated in stomach and small intestinal GISTs, respectively. Aberrant regulation of these gene products was initially detected at the mRNA level and was later confirmed at the protein level using specific antibodies. Presently, any global approach to protein expression cannot uncover the whole proteome in a quantitative and reproducible way. The continuing efforts to improve the sensitivity of proteomic modalities have enabled the uncovering of several thousands of proteins with posttranslational modifications (24, 44, 45). We believe that such efforts will overcome some of the inherent limitations of proteomics and lead to a more detailed understanding of the disease mechanisms and to novel therapeutic strategies in the near future.

In conclusion, we identified a possible correlation of 43 protein variants corresponding to 25 distinct gene products with variables of clinical interest in GIST and validated pfetin expression using a specific antibody. From this study, pfetin expression is predictive of metastasis and survival of patients with GISTs and, as such, may be used in clinical practice to improve existing therapeutic strategies. Assessment of the prognostic power of the combined use of pfetin and the other 24 proteins as well as more extensive validation of pfetin using additional samples are now under way in our laboratory.

Acknowledgments

We thank Kiyoaki Nomoto, Chizu Kina, and Sachiko Miura for their excellent technical support in the immunohistochemical study, and Kano Nishiyama and Yukiko Fujie in electrophoresis.

References

1. Joensuu H, Kindblom LG. Gastrointestinal stromal tumors-a review. Acta Orthop Scand Suppl 2004;75: 62–71.
2. Miettinen M, El-Rifai W, HL Sobin L, Lasota J. Evaluation of malignancy and prognosis of gastrointestinal stromal tumors: a review. Hum Pathol 2002;33: 478–83.
3. Corless CL, Fletcher JA, Heinrich MC. Biology of gastrointestinal stromal tumors. J Clin Oncol 2004; 22:3813–25.
4. Heinrich MC, Rubin BP, Longley BJ, Fletcher JA. Biology and genetic aspects of gastrointestinal stromal tumors: KIT activation and cytogenetic alterations. Hum Pathol 2002;33:484–95.
5. Miettinen M, Majidi M, Lasota J. Pathology and diagnostic criteria of gastrointestinal stromal tumors (GISTs): a review. Eur J Cancer 2002;38 Suppl 5: S39–51.
6. Demetri GD, von Mehren M, Blanke CD, et al. Efficacy and safety of imatinib mesylate in advanced gastrointestinal stromal tumors. N Engl J Med 2002;347: 472–80.
7. van Oosterom AT, Judson I, Verweij J, et al. Safety and efficacy of imatinib (STI571) in metastatic gastrointestinal stromal tumours: a phase I study. Lancet 2001;358:1421–3.
8. Heinrich MC, Corless CL, Blanke CD, et al. Molecular correlates of imatinib resistance in gastrointestinal stromal tumors. J Clin Oncol 2006;24:4764–74.
9. Debiec-Rychter M, Sciot R, Le Cesne A, et al. KIT mutations and dose selection for imatinib in patients with advanced gastrointestinal stromal tumours. Eur J Cancer 2006;42:1093–103.
10. Debiec-Rychter M, Dumez H, Judson I, et al. Use of c-KIT/PDGFRA mutational analysis to predict the clinical response to imatinib in patients with advanced gastrointestinal stromal tumours entered on phase I and II studies of the EORTC Soft Tissue and Bone Sarcoma Group. Eur J Cancer 2004;40: 689–95.
11. Schneider-Stock R, Boltze C, Lasota J, et al. Loss of p16 protein defines high-risk patients with gastrointestinal stromal tumors: a tissue microarray study. Clin Cancer Res 2005;11:638–45.
12. Schneider-Stock R, Boltze C, Lasota J, et al. High prognostic value of p16INK4 alterations in gastrointestinal stromal tumors. J Clin Oncol 2003;21: 1688–97.
13. Rumessen JJ, Peters S, Thuneberg L. Light- and electron microscopical studies of interstitial cells of Cajal and muscle cells at the submucosal border of human colon. Lab Invest 1993;68:481–95.
14. Tornillo L, Duchini G, Carafa V, et al. Patterns of gene amplification in gastrointestinal stromal tumors (GIST). Lab Invest 2005;85:921–31.
15. El-Rifai W, Sarlomo-Rikala M, Andersson LC, Knuutila S, Miettinen M. DNA sequence copy number changes in gastrointestinal stromal tumors: tumor progression and prognostic significance. Cancer Res 2000;60:3899–903.
16. Kang HJ, Nam SW, Kim H, et al. Correlation of KIT and platelet-derived growth factor receptor α mutations with gene activation and expression profiles in gastrointestinal stromal tumors. Oncogene 2005;24: 1066–74.
17. Koon N, Schneider-Stock R, Sarlomo-Rikala M, et al. Molecular targets for tumour progression in gastrointestinal stromal tumours. Gut 2004;53:235–40.
18. Antonescu CR, Viale A, Sarran L, et al. Gene expression in gastrointestinal stromal tumors is distinguished by KIT genotype and anatomic site. Clin Cancer Res 2004;10:3282–90.
19. Petricoin EF, Ardekani AM, Hitt BA, et al. Use of proteomic patterns in serum to identify ovarian cancer. Lancet 2002;359:572–7.
20. Suehara Y, Kondo T, Fujii K, et al. Proteomic signatures corresponding to histological classification and grading of soft-tissue sarcomas. Proteomics 2006;6: 4402–9.
21. Chen G, Gharib TG, Wang H, et al. Protein profiles associated with survival in lung adenocarcinoma. Proc Natl Acad Sci U S A 2003;100:13537–42.
22. Okano T, Kondo T, Fujii K, et al. Proteomic signature corresponding to the response to gefitinib (Iressa, ZD1839), an epidermal growth factor receptor (EGFR) tyrosine kinase inhibitor, and mutation in EGFR in lung adenocarcinoma. Clin Cancer Res 2007;13:799–805.
23. Orntoft TF, Thykjaer T, Waldman FM, Wolf H, Celis JE. Genome-wide study of gene copy numbers, transcripts, and protein levels in pairs of non-invasive and invasive human transitional cell carcinomas. Mol Cell Proteomics 2002;1:37–45.
24. Varambally S, Yu J, Laxman B, et al. Integrative genomic and proteomic analysis of prostate cancer reveals signatures of metastatic progression. Cancer Cell 2005;8:393–406.
25. Resendes BL, Kuo SF, Robertson NG, et al. Isolation from cochlea of a novel human intronless gene with predominant fetal expression. J Assoc Res Otolaryngol 2004;5:185–202.
26. Stankey RH LA. Pathology and Genetics of Tumours of the Digestive System. Lyon: IARC Press; 2000.
27. Hasegawa T, Matsuno Y, Shimoda T, Hirohashi S. Gastrointestinal stromal tumor: consistent CD117 immunostaining for diagnosis, and prognostic classification based on tumor size and MIB-1 grade. Hum Pathol 2002;33:669–76.
28. Unlu M, Morgan ME, Minden JS. Difference gel electrophoresis: a single gel method for detecting changes in protein extracts. Electrophoresis 1997;18:2071–7.
29. Yokoo H, Kondo T, Fujii K, Yamada T, Todo S, Hirohashi S. Proteomic signature corresponding to α fetoprotein expression in liver cancer cells. Hepatology 2004;40:609–17.
30. Okano T, Kondo T, Kakisaka T, et al. Plasma proteomics of lung cancer by a linkage of multi-dimensional liquid chromatography and two-dimensional difference gel electrophoresis (2D-DIGE). Proteomics 2006;6:3938–48.
31. Yoshida Y, Shibata T, Kokubu A, et al. Mutations of the epidermal growth factor receptor gene in atypical adenomatous hyperplasia and bronchioloalveolar carcinoma of the lung. Lung Cancer 2005;50:1–8.
32. Kaplan EL, Meier P. Nonparametric estimation from incomplete observations. J Am Stat Assoc 1958;53: 457–81.
33. Kang HJ, Koh KH, Yang E, et al. Differentially expressed proteins in gastrointestinal stromal tumors with KIT and PDGFRA mutations. Proteomics 2006; 6:1151–7.
34. Molina H, Horn DM, Tang N, Mathivanan S, Pandey A. Global proteomic profiling of phosphopeptides using electron transfer dissociation tandem mass spectrometry. Proc Natl Acad Sci U S A 2007;104:2199–204.
35. Matsuoka S, Ballif BA, Smogorzewska A, et al. ATM and ATR substrate analysis reveals extensive protein networks responsive to DNA damage. Science 2007;316:1160–6.
36. Lasota J, Jasinski M, Sarlomo-Rikala M, Miettinen M. Mutations in exon 11 of c-Kit occur preferentially in malignant versus benign gastrointestinal stromal tumors and do not occur in leiomyomas or leiomyosarcomas. Am J Pathol 1999;154:53–60.
37. Ernst SI, Hubbs AE, Przygodzki RM, Emory TS, Sobin LH, O'Leary TJ. KIT mutation portends poor

prognosis in gastrointestinal stromal/smooth muscle tumors. Lab Invest 1998;78:1633–6.

38. Hirota S, Isozaki K, Nishida T, Kitamura Y. Effects of loss-of-function and gain-of-function mutations of c-kit on the gastrointestinal tract. J Gastroenterol 2000; 35 Suppl 12:75–9.

39. Wardelmann E, Losen I, Hans V, et al. Deletion of Trp-557 and Lys-558 in the juxtamembrane domain of the c-kit protooncogene is associated with metastatic behavior of gastrointestinal stromal tumors. Int J Cancer 2003;106:887–95.

40. Lasota J, Dansonka-Mieszkowska A, Stachura T, et al. Gastrointestinal stromal tumors with internal tandem duplications in 3′ end of KIT juxtamembrane domain occur predominantly in stomach and generally seem to have a favorable course. Mod Pathol 2003; 16:1257–64.

41. Antonescu CR, Sommer G, Sarran L, et al. Association of KIT exon 9 mutations with nongastric primary site and aggressive behavior: KIT mutation analysis and clinical correlates of 120 gastrointestinal stromal tumors. Clin Cancer Res 2003;9: 3329–37.

42. Montgomery E, Abraham SC, Fisher C, et al. CD44 loss in gastric stromal tumors as a prognostic marker. Am J Surg Pathol 2004;28:168–77.

43. Nishitani A, Hirota S, Nishida T, et al. Differential expression of connexin 43 in gastrointestinal stromal tumours of gastric and small intestinal origin. J Pathol 2005;206:377–82.

44. Klose J, Nock C, Herrmann M, et al. Genetic analysis of the mouse brain proteome. Nat Genet 2002;30: 385–93.

45. Kondo T, Hirohashi S. Application of highly sensitive fluorescent dyes (CyDye DIGE Fluor saturation dyes) to laser microdissection and two-dimensional difference gel electrophoresis (2D-DIGE) for cancer proteomics. Nat Protoc 2006;1: 2940–56.

Bone Marrow Transplantation (2008) 41, 1067–1068

www.nature.com/bmt

LETTER TO THE EDITOR

Segregated graft-versus-tumor effect between CNS and non-CNS lesions of Ewing's sarcoma family of tumors

Bone Marrow Transplantation (2008) **41**, 1067–1068; doi:10.1038/bmt.2008.26; published online 10 March 2008

For patients with the localized Ewing's sarcoma family of tumors (ESFT), first-line multimodal treatment, including intensive multi-agent chemotherapy, local radiation therapy and surgery, produces 70–75% of the long-term survival rate.[1,2] However, once patients relapse, there is no effective treatment that yields a 5-year survival rate exceeding 20%, even with high-dose chemotherapy (HDC) with autologous stem cell rescue.[3,4] Therefore, a new and more effective treatment approach is clearly needed for this population. Several reports have described patients with ESFT who had bone marrow metastases and underwent allogeneic SCT instead of autologous SCT,[5] including a rare patient who exhibited evidence of a graft-versus-tumor (GVT) effect.[6] To accumulate further knowledge, we report the case of a patient with recurrent ESFT who responded to allogeneic SCT from a sibling donor. A unique aspect of this case was that the manifestation of the GVT effect differed in different organs, with involvement of central nervous system (CNS) and non-CNS lesions. The GVT effect is rare in CNS diseases.

A 28-year-old woman was diagnosed with ESFT of the right chest wall. The tumor size was $10 \times 11 \times 8$ cm and no metastases were shown on computed tomography (CT) or bone scans. Histology revealed small, round cells positive for the cell-surface glycoprotein CD99 and negative for desmin, myoD1, S100 protein, CD45 and CD30. Primary treatment comprised of two courses of chemotherapy with vincristine, doxorubicin and cyclophosphamide (VDC), followed by two courses of ifosfamide, and then HDC with thiotepa 300 mg/m^2 for 2 days and etoposide 300 mg/m^2 for 3 days with autologous peripheral blood stem cell rescue. Local radiation therapy with 50 Gy X-ray was also administered. The patient remained well without evidence of recurrent disease until 20 months after the autologous SCT, when she presented with chest pain and a recurrent tumor in the original site was observed on CT scanning (Figure 1a). After four courses of re-induction chemotherapy, including one course of VDC, one course of ifosfamide and etoposide (IE), and two courses of irinotecan, and HDC consisting of etoposide 200 mg/m^2 for 4 days and melphalan 90 mg/m^2 for 2 days with autologous peripheral blood stem cell rescue, she achieved partial remission (Figure 1b). The patient then entered a phase I/II clinical trial of reduced-intensity allogeneic SCT. After

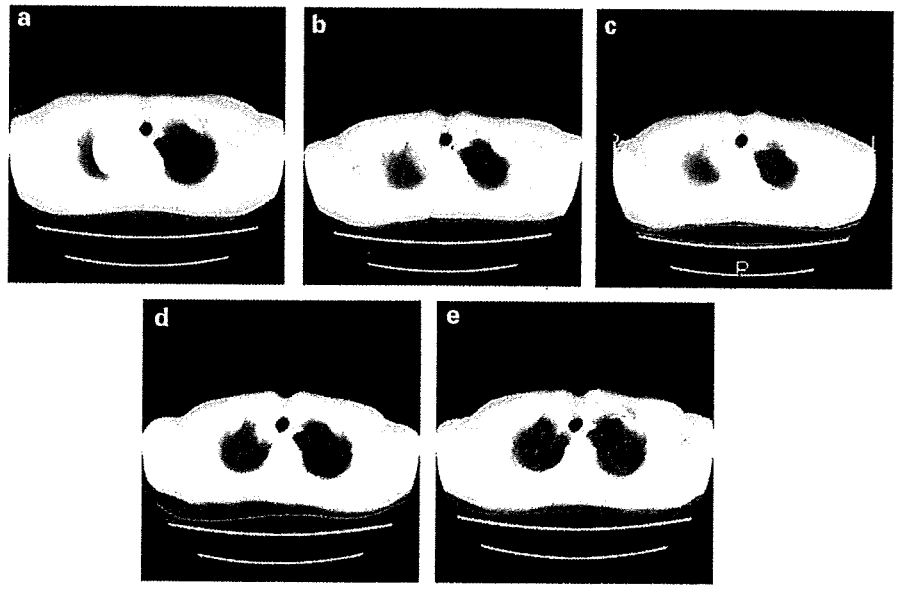

Figure 1 (a) Computed tomography (CT) images of a primitive neuroectodermal tumor in the apical lesion on relapse after autoperipheral blood SCT. (b) After four courses of chemotherapy, the patient achieved partial remission. A CT scan taken 1 month after the allogeneic SCT, the tumor size was almost no change (c), but 4 months after, it showed 50% reduction of the apical tumor (d). CR was confirmed at 8 months (e).

preconditioning with busulfan (4 mg/kg/day, orally from day −4 to day −3) and fludarabine (30 mg/m^2/day, intravenously from day −8 to day −3), peripheral blood cells containing 2.4 × 10^6/kg CD34$^+$ cells from her HLA-matched sister were infused. Prophylactic immunosuppression with cyclosporine-A was started on day −1. Her post transplant course was uncomplicated, except for transient grade 1 GVHD of the skin, which began on day +64 and resolved by day +67 without any specific treatment. Cyclosporine-A was tapered from day +70 and discontinued on day +106. A CT scan taken 1 month after the allogeneic SCT when the tumor size was almost unchanged (Figure 1c), but 4 months later, there was 50% reduction of the apical tumor (Figure 1d). CR was confirmed at 8 months (Figure 1e). The patient had headache and was found to have CNS disease on magnetic resonance imaging at 14 months. She died of the disease 5 months after the second relapse. The patient relapsed after initial treatment including HDC with autologous stem cell support, but thereafter, the tumor disappeared coincidently with the occurrence of GVHD, and at least for the primary lesion, the regression period exceeded the period of initial remission. Hence, a graft-versus-ESFT effect seems likely.

In this case, we followed the patient mainly by CT scanning. Although the CT findings showed the tumor status fairly well, they could not provide information regarding viability of the residual tumor. In this regard, PET scanning would be very helpful.

Interestingly, although the GVT effect was exerted in the primary lesion in the chest wall, it was not effective for the prevention of CNS recurrence in this case. The speculated reason for this observation is that the CNS is essentially an immunologically privileged site and theoretically, donor-derived immunocompetent cells carrying the GVT effect mechanism cannot cross the blood–brain barrier.[7] Hence, the application of additional therapeutic intervention to the CNS might become necessary after any systemic manifestations of a GVT effect.

A Hosono[1], A Makimoto[1], A Kawai[2] and Y Takaue[3]
[1]*Division of Pediatric Oncology, National Cancer Center Hospital, Tokyo, Japan;*
[2]*Division of Orthopedic Surgery, National Cancer Center Hospital, Tokyo, Japan and*
[3]*Division of Hematopoietic Stem Cell Transplantation, National Cancer Center Hospital, Tokyo, Japan*
E-mail: ahosono@ncc.go.jp

References

1 Marina NM, Pappo AS, Parham DM, Cain AM, Rao BN, Poquette CA *et al.* Chemotherapy dose-intensification for pediatric patients with Ewing's family of tumors and desmoplastic small round cell tumor: a feasibility study at St Jude Children's Research Hospital. *J Clin Oncol* 1999; **17**: 180–190.
2 Grier HE, Krailo MD, Tarbell NJ, Link MP, Fryer CJ, Pritchard DJ *et al.* Addition of ifosfamide and etoposide to standard chemotherapy for Ewing's sarcoma and primitive neuroectodermal tumor of bone. *N Engl J Med* 2003; **348**: 694–701.
3 Barker LM, Pendergrass TW, Sanders JE, Hawkins DS. Survival after recurrence of Ewing's sarcoma family of tumors. *J Clin Oncol* 2005; **23**: 4354–4362.
4 Galindo CR, Billups CA, Kun LE, Rao BN, Pratt CB, Merchant TE *et al.* Survival after recurrence of Ewing tumors. *Cancer* 2002; **94**: 561–569.
5 Burdach S, Kaick BV, Laws HJ, Ahrens S, Haase R, Korholz D *et al.* Allogenic and autologous stem-cell transplantation in advanced Ewing tumors. *Ann Oncol* 2000; **11**: 1451–1462.
6 Koscielniak E, Wieltsch U, Treuner J, Winker P. Graft-versus-Ewing sarcoma effect and long-term remission induced by haploidentical stem-cell transplantation in a patient with relapse of metastatic disease. *J Clin Oncol* 2005; **23**: 242–248.
7 Carson CM, Sutcliffe JG. Balancing function vs. self-defense: the CNS as an active regulator of immune response. *J Neurosci Res* 1999; **55**: 1–8.

Clin Orthop Relat Res (2008) 466:2099–2106
DOI 10.1007/s11999-008-0330-4

SYMPOSIUM: MOLECULAR GENETICS IN SARCOMA

Global Protein-expression Analysis of Bone and Soft Tissue Sarcomas

Akira Kawai MD, PhD, Tadashi Kondo MD, PhD, Yoshiyuki Suehara MD, PhD, Kazutaka Kikuta MD, Setsuo Hirohashi MD, PhD

Published online: 6 June 2008

Abstract Analysis of global protein expression, an approach known as expression proteomics, can offer important clues for understanding tumor biology that cannot be obtained by other approaches (e.g., genome or transcriptome analysis). Using two-dimensional difference gel electrophoresis (2D-DIGE) and mass spectrometry, we performed global protein expression studies of bone and soft tissue sarcomas to develop novel diagnostic and therapeutic biomarkers and allow molecular classification of the tumors. Among 1500 protein variants identified in the two-dimensional gel, 67 proteins correctly distinguished the eight subtypes of 99 histologically classified soft tissue sarcomas. Hierarchical clustering demonstrated leiomyosarcoma and MFH shared a similar protein expression profile, and clear cell sarcoma, synovial sarcoma, and MPNST could be grouped according to their protein expression patterns. Pleomorphic leiomyosarcoma and MFH showed similar tropomyosin isoform expression patterns. Patients with gastrointestinal stromal tumors expressing pfetin protein had better survival than those whose tumors lacked it. We identified 10 protein spots associated with the chemosensitivity of osteosarcoma to preoperative chemotherapy. These 10 spots could be new diagnostic and prognostic markers for osteosarcoma and new therapeutic targets for the disease. Proteomic analysis using 2D-DIGE provides novel information on the biology of bone and soft tissue sarcomas that could be used to diagnosis and treat these tumors.
Level of Evidence: Level II, diagnostic study. See the Guidelines for Authors for a complete description of levels of evidence.

This work was supported by a grant from the Ministry of Health, Labor and Welfare (AK, TK), a grant from the Ministry of Education, Science, Sports, and Culture (AK), and a grant from the Program for Promotion of Fundamental Studies in Health Sciences of the National Institute of Biomedical Innovation of Japan (TK).
Each author certifies that his or her institution has approved the human protocol for this investigation and that all investigations were conducted in conformity with ethical principles of research.

A. Kawai (✉), Y. Suehara, K. Kikuta
Division of Orthopaedic Surgery, National Cancer Center Hospital, 5-1-1 Tsukiji, Chuo-ku, Tokyo, Japan
e-mail: akawai@ncc.go.jp

T. Kondo, S. Hirohashi
Proteome Bioinformatics Project, National Cancer Center Research Institute, Tokyo, Japan

Y. Suehara
Department of Orthopaedic Surgery, Juntendo University School of Medicine, Tokyo, Japan

Introduction

Over the past three decades, advances in diagnostic modalities and treatment methods have substantially improved the survival rate and postoperative limb function of patients with bone and soft tissue sarcomas [5, 10, 20, 27, 40]. Wide excision of tumors in conjunction with multiagent chemotherapy now provides 5-year disease-specific survivals ranging from 60% to 80% in patients with localized high-grade sarcomas [2, 5, 27]. Despite this success, the outcomes of patients who have metastatic disease at diagnosis or those with tumors showing a poor response to chemotherapy are still unsatisfactory (5-year disease-specific survival rates, 20%–40%), even with dose-intensive or high-dose chemotherapy [9, 18, 19, 33]. For improving the prognosis of patients with these difficult-to-treat sarcomas, it is imperative to develop new targeted therapeutic strategies based on an understanding of the

biologic mechanisms underlying the metastasis and chemoresistance of these tumors.

Recent development of high-throughput screening techniques has allowed global investigations of the molecular backgrounds associated with the clinicopathologic characteristics of tumors. A DNA microarray-based approach allows the screening of several thousand mRNAs in bone and soft tissue sarcomas and can identify the genes relevant to their histologic diagnosis, clinical features, and chemosensitivity [39]. Using an oligonucleotide microarray approach, Nakayama et al. [31] analyzed gene expression in 105 soft tissue sarcoma samples and reclassified malignant fibrous histiocytoma (MFH), which has a wide variety of clinicopathologic features, into pleomorphic subtypes of other distinct types of sarcomas. Based on gene-expression profiles, Ochi et al. [34] identified 60 genes whose expression levels were likely correlated with the chemosensitivity of osteosarcomas. Mintz et al. [29] reported 104 genes were differentially expressed between chemotherapy-sensitive and -resistant osteosarcomas.

Although much evidence suggests genetic abnormalities play a primary role in the development of tumors, there is also evidence for the effects of aberrations that cannot be detected solely by genome (DNA sequencing) or transcriptome (measurement of all mRNA in a population of cells) analysis: posttranslational modifications of proteins such as phosphorylation, glycosylation, and degradation, are aberrantly regulated in many types of cancers and cannot be predicted by DNA sequencing or measurement of mRNA expression. It has become evident there is considerable discrepancy between expression of mRNA and that of protein [4, 12]. Further, proteins are more directly linked to aberrant tumor phenotypes. These difficulties underline the potential advantages of monitoring protein expression in a global manner, an approach known as expression proteomics. In addition, the results obtained from proteomic studies will be more easily applicable to the clinical field with the use of specific antibodies.

We have performed global protein expression studies using our original high-throughput two-dimensional difference gel electrophoresis (2D-DIGE) system on several types of tumors [21, 22]. This approach has proven useful for classifying soft tissue sarcomas at the protein expression level and for identifying novel diagnostic and prognostic markers [37]. Biomarkers specifically expressed in a specific subgroup of tumors can facilitate a risk-adopted tailored medical treatment. Examination of the markers may allow the identification of a high-risk patient group that may benefit from adjuvant therapy, whereas it may also help spare low-risk patients unnecessary treatment. Moreover, specifically expressed molecules or associated pathways could be crucial molecular targets to allow for more selective therapeutic intervention.

We report our approach for identifying biomarkers that associate with clinicopathologic features of bone and soft tissue sarcomas using global protein expression analysis.

Materials and Methods

We performed protein expression profiling for 99 soft tissue sarcomas: 28 MFHs, 19 rhabdomyosarcomas, 12 synovial sarcomas, 10 leiomyosarcomas, 10 myxoid liposarcomas, nine gastrointestinal stromal tumors (GIST), six clear cell sarcomas, and five malignant peripheral nerve sheath tumors (MPNST) using 2D-DIGE. We used the term "MFH" to describe tumors diagnosed as storiform and pleomorphic-type MFH that showed predominant pleomorphic features without any findings of a specific type of differentiation. All tumor samples were obtained from patients treated at the National Cancer Center Hospital (Tokyo, Japan). We snap-froze fresh-frozen samples in liquid nitrogen immediately after resection or biopsy sampling before any treatment and stored them at −80°C until use. Tumor samples for immunohistochemical analysis were preserved in archival paraffin-embedded tissue blocks. This study was approved by the Institutional Review Board and conducted according to tenets of the Declaration of Helsinki.

Protein expression profiles were studied by 2D-DIGE as described previously [21, 22]. For protein extraction, the frozen samples were homogenized with urea lysis buffer (6 M urea, 2 M thiourea, 3% CHAPS, 1% Triton X-100). After centrifugation at 15,000 rpm for 30 minutes, the supernatant was used for studies. A mixture of all the experimental samples was used as an internal control sample. The internal control and individual samples were labeled with fluorescent dyes with different excitation and emission wavelengths (CyDye DIGE Fluor saturation dye; Amersham Biosciences, Little Chalfont, Buckinghamshire, UK): Cy3 for the internal control and Cy5 for the individual samples. The Cy3-labeled control sample and the Cy5-labeled individual sample were mixed and coseparated by two-dimensional polyacrylamide gel electrophoresis. The first-dimensional separation was performed using an immobilized pH gradient gel (length 24 cm, p*I* range 3-10; Amersham Biosciences) in accordance with the manufacturer's recommended protocol. The immobilized pH gradient gels were then equilibrated and transferred to 9% to 16% polyacrylamide gradient gels measuring 24 cm × 20 cm. The gels were run in an Ettan Dalt II system (Amersham Biosciences) at 18 W and 18°C for 15 hours. Each sample was run on triplicate gels and the average spot intensities were calculated for quantitative analysis.

After electrophoresis, the gels were scanned at appropriate wavelengths for Cy3 and Cy5 using a 2-D 2920

MasterImager (Amersham Biosciences) [21, 22]. The ratio of Cy5 intensity to Cy3 intensity was calculated for all spots in each gel with DeCyder software (Amersham Biosciences) to obtain the standardized spot intensities. Because the Cy3 image represents the internal standard sample, this standardization procedure eliminates gel-to-gel differences. Approximately 1500 protein spots were visualized by laser scanning (Fig. 1). The standardized spot intensities were logarithmically transformed and analyzed with the data-mining package Impressionist (GeneData, Basel, Switzerland).

We identified informative proteins using a support vector machine algorithm with leave-one-out crossvalidation. The classification performance of a candidate classifier was evaluated by multivariate analysis, including principal component analysis and hierarchical clustering. Proteins corresponding to the spots of interest were identified by mass spectrometric analysis using a matrix laser desorption/absorption/ionization (MALDI) time of flight mass spectrometer. Protein identification and differential expression were confirmed by Western blotting using specific antibodies.

Immunohistochemical analysis was performed according to the streptavidin-biotin peroxidase method using a Strept ABC Complex/HRP kit (DAKO, Tokyo, Japan) on formalin-fixed paraffin-embedded tissues. Rabbit polyclonal antibody against pfetin was kindly provided by Dr Morton [35]. Two reviewers (YS, AK) reviewed the results of immunohistochemical staining in a blinded fashion regarding the clinical data.

We calculated tumor-specific survival time from the first resection of primary tumor to death from tumor-specific causes. Patients who died of causes unrelated to the disease were censored at the time of death. All time to event end points were computed using the Kaplan and Meier method. We used the log-rank test to determine differences in survival between subgroups. We used the Cox proportional hazards regression to analysis differences in survival after adjusting for potentially confounding variables (site, size, differentiation and pfetin).

To identify markers associated with osteosarcoma chemosensitivity, we analyzed the protein expression profiles of 23 biopsy samples of typical osteosarcoma (conventional central high-grade osteosarcomas that had developed in long tubular bones in patients with a mean age of 18 years). All the patients received standard pre- and postoperative chemotherapy consisting of high-dose methotrexate, cisplatin, doxorubicin, and ifosfamide. The histologic effects of preoperative chemotherapy according to the Huvos grading system [36] were Grade I in seven cases, Grade II in seven, Grade III in six, and Grade IV in three. We compared the protein expression profiles of two distinct groups; nine samples from patients showing a good response to preoperative chemotherapy (greater than 90% tumor necrosis; Huvos Grades III and IV) and seven samples from patients showing a poor response (less than 50% tumor necrosis; Huvos Grade I).

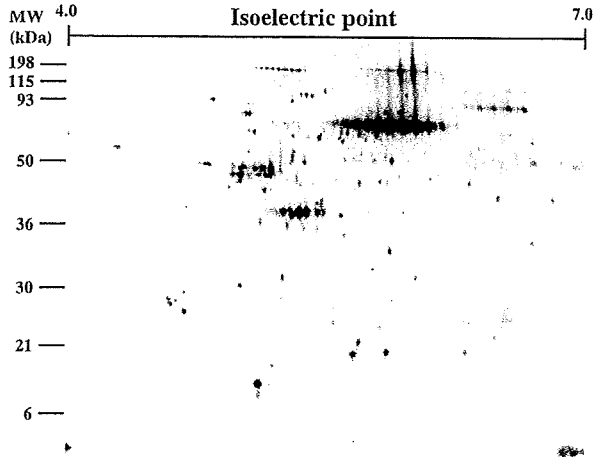

Fig. 1 Representative two-dimensional image of Cy5-labeled proteins of osteosarcoma. Approximately 1500 protein spots are visualized by laser scanning. Proteins corresponding to the spots of interest were picked up and identified by mass spectrometric analysis.

Results

Hierarchical clustering using all 1500 protein spots did not classify the tumors exactly in accordance with the histologic classification. To examine the possible differences in protein expression between different types of sarcoma, we selected 67 proteins whose expression was associated with the existing histologic classification by using a support vector machine algorithm (Fig. 2). All the tumors were separable into six clusters. Myxoid liposarcomas and rhabdomyosarcomas formed tight clusters on two distinct dendrogram branches. The third and fourth clusters mostly comprised a mixture of leiomyosarcomas and MFHs. The third cluster contained a large proportion of leiomyosarcomas, whereas the fourth cluster contained mostly MFHs together with two cases of pleomorphic leiomyosarcoma and a case of CCS. GISTs formed a distinct fifth cluster. The sixth cluster comprised three different types of sarcomas (CCS, synovial sarcoma, and MPNST) and three outlier cases.

Using supervised analysis of pleomorphic and conventional leiomyosarcomas, we found tropomyosin isoforms were responsible for leiomyosarcoma subtypes. Conventional leiomyosarcoma expressed mainly tropomyosin isoforms 1 and 2, whereas pleomorphic leiomyosarcoma largely expressed tropomyosin isoforms 3 and 4 (Fig. 3). MFH shared an expression pattern of tropomyosin isoforms

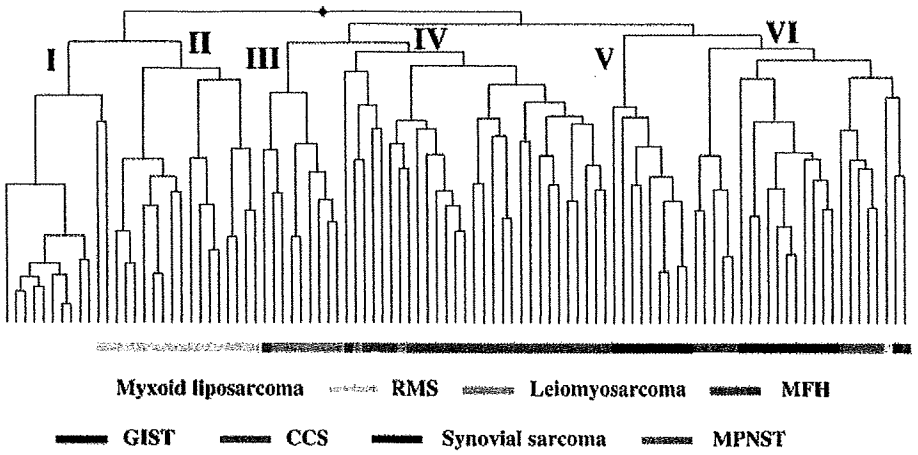

Fig. 2 Hierarchical classification of the 99 soft tissue sarcomas using the selected 67 proteins. The dendrogram shows the degree of similarity of protein expression pattern between the tumors. The shorter the branches, the more similar the two joined tumors. Most tumors formed tight clusters corresponding to their histology except leiomyosarcoma and malignant fibrous histiocytoma. RMS = rhabdomyosarcoma; MFH = malignant fibrous histiocytoma; GIST = gastrointestinal stromal tumor; MPNST = malignant peripheral nerve sheath tumor.

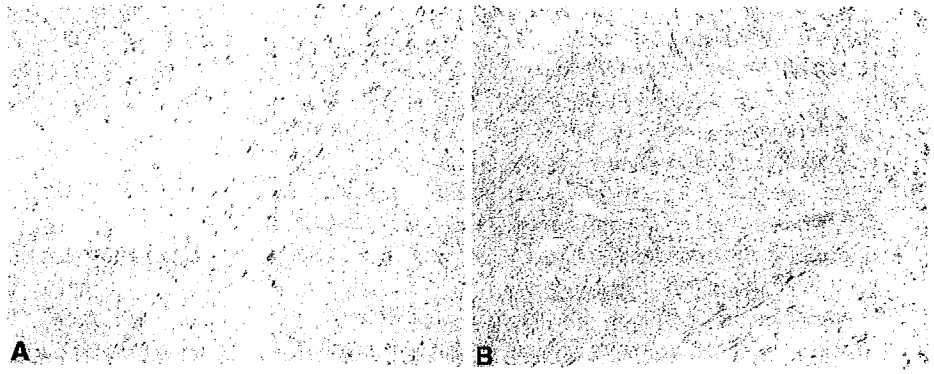

Fig. 3A–B Immunohistochemical staining of tropomyosin isoform type 4. Representative photomicrographs of (A) conventional leiomyosarcoma and (B) pleomorphic leiomyosarcoma. Tropomyosin isoform 4 is highly expressed in pleomorphic leiomyosarcoma, but not in conventional leiomyosarcoma (stain, immunohistochemical staining for tropomyosin isoform 4; original magnification, ×200).

(mainly types 3 and 4) similar to that of pleomorphic leiomyosarcoma.

By comparing the protein expression profiles of two distinct groups of GISTs—pathologically high-risk and clinically aggressive cases and pathologically low- or intermediate-risk and clinically indolent cases—we identified 43 protein spots whose expression differed (Wilcoxon test, $p < 0.001$) between the two groups. Mass spectrometric identification demonstrated the 43 spots corresponded to 25 distinct gene products, eight of which were derived from a potassium channel protein, pfetin. Western blotting and real-time PCR suggested pfetin expression inversely correlated ($p < 0.0001$) with the development of metastasis. Immunohistochemical analysis revealed patients with tumors expressing pfetin protein had better ($p < 0.0001$) tumor-specific survival than those with tumors lacking pfetin expression (Fig. 4).

By comparing the protein expression profiles (1465 protein spots) of two distinct groups of osteosarcoma biopsy samples—a chemosensitive group (good responders; Huvos

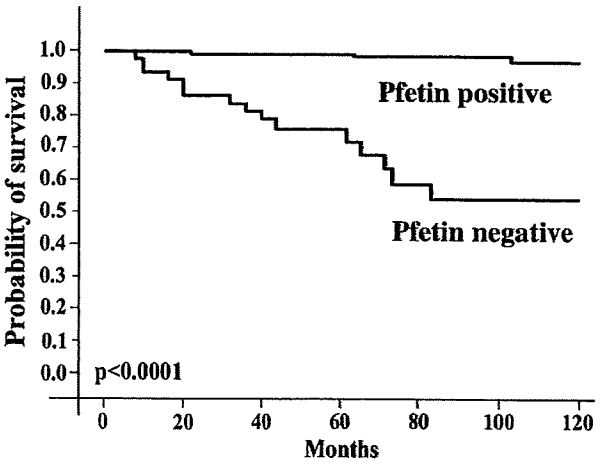

Fig. 4 Tumor-specific survival of 210 patients with M0 gastrointestinal stromal tumors according to the expression of pfetin protein in the primary tumor samples examined by immunohistochemistry. Patients with tumors expressing pfetin (n = 171) had better ($p < 0.0001$) survival (5-year survival, 97.2%) than those with tumors lacking pfetin expression (n = 39) (5-year survival, 76.5%).

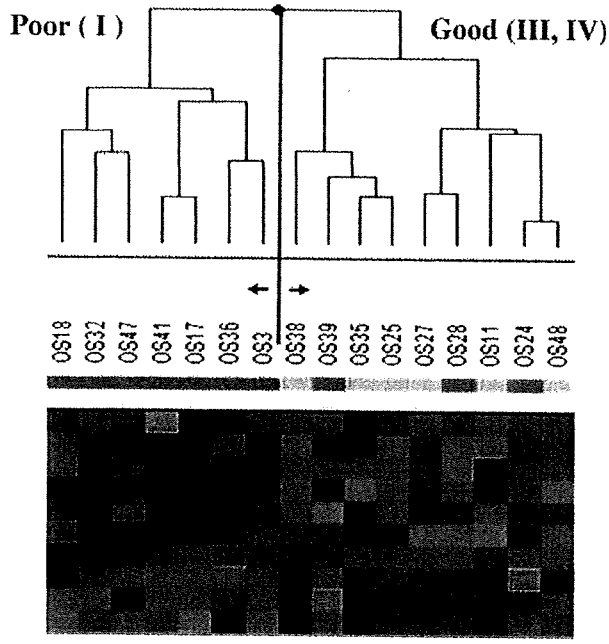

Fig. 5 Expression pattern of the 10 protein spots that discriminate good responders (Huvos Grades III, IV) from poor responders (Huvos Grade I) among 16 patients with osteosarcoma. Horizontal rows represent individual protein spots, and vertical columns represent individual samples. Each cell in the matrix represents the expression level of a single protein spot in a single sample. Red indicates overexpression relative to the expression of the control sample, whereas green indicates underexpression. There are seven spots that are overexpressed in poor responders and three spots overexpressed in good responders.

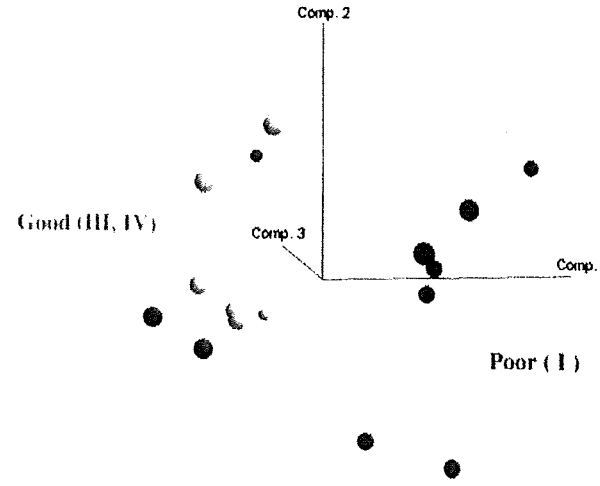

Fig. 6 Principal component analysis of the 16 osteosarcomas on the basis of the expression profiles of the 10 selected protein spots. It accurately classifies the osteosarcoma samples into either good responders (Huvos Grades III, IV) or poor responders (Huvos Grade I).

Grades III and IV) versus a chemoresistant group (poor responders; Huvos Grade I)—we identified 10 protein spots whose expression differed (Wilcoxon test, $p < 0.05$) between the two groups (Fig. 5). Among these 10 spots, the expression levels of seven spots were higher and those of three spots were lower in poor responders compared with good responders. Principal component analysis accurately divided the osteosarcoma samples into good responder and poor responder groups based on the expression levels of the 10 selected classifiers (Fig. 6).

Discussion

Many lines of evidence have revealed genetic alterations such as activation of oncogenes, inactivation of tumor suppressor genes, and chromosomal translocations play a primary role in the development of bone and soft tissue sarcomas [6, 16, 24]. These genetic alterations initiate changes in a series of signal transduction pathways and develop malignant tumor cells. Although the initial changes occur at the DNA level, all the effects are ultimately expressed as the changes of the protein content. Proteins are considered the hallmark of genetic alterations. Global mRNA expression studies are often performed to follow these changes [29, 30–34]. However, recent comparative studies of mRNA and protein expression in tumor cells revealed only a subset of mRNA correlated with protein abundance [4, 12]. Moreover, posttranslational modifications, which play important roles in tumor biology, cannot be predicted only by mRNA examinations. These limitations of mRNA expression studies underline the potential advantages of monitoring protein expression in a global manner, an approach known as expression proteomics. Recently, using MALDI MS tissue profiling, Holt et al. [14] reported protein peaks that were differentially expressed in high-grade and low-grade soft tissue sarcomas. Among several proteomic technologies, 2D-DIGE has advantages that make it possible to examine hundreds of proteins simultaneously estimating their expression and posttranslational modifications quantitatively [21, 22]. Applications of sensitive fluorescent dyes and laser scanning made it possible to execute large-scale proteomics in a more efficient, accurate, and reproducible way. In the present study, we examined the protein expression profiles of a diverse group of bone and soft tissue sarcomas in relation to their clinicopathologic features using the 2D-DIGE technique.

A limitation of the current 2D-DIGE is the thoroughness of the analysis. Although the method reveals global expression profiles of more than 1000 protein spots quantitatively, it cannot uncover proteins expressed in very low levels. Compared with the cDNA microarray analysis (20,000 probe sets), the sensitivity of the current 2D-DIGE analysis (1500 spots) is unsatisfactory. We are now trying

to improve the sensitivity of 2D-DIGE using a large-format polyacrylamide gel (24 cm × 38 cm) for two-dimensional polyacrylamide gel electrophoresis. Preliminary results demonstrated more protein spots (5000 spots) are quantitatively detected in the large-format two-dimensional gels. We believe such efforts may overcome some of the inherent limitations of the proteomics.

We found 67 proteins correctly distinguished the eight subtypes of 99 soft tissue sarcomas according to their histologic classification. Hierarchical clustering demonstrated leiomyosarcoma and MFH shared a similar protein expression profile, some of which was not distinguishable on the basis of protein expression, and that clear cell sarcoma, synovial sarcoma, and MPNST were grouped according to their protein expression patterns. These results were generally consistent with previous reports based on histologic and transcriptome analyses [7, 13, 19, 25, 30–32].

Using immunohistochemical analysis, Hasegawa et al. [13] demonstrated a large subset of MFH expressed poorly differentiated smooth muscle or myofibroblastic features and should be regarded as pleomorphic leiomyosarcoma or pleomorphic myofibrosarcoma. Fletcher et al. [7] examined 100 cases of so-called MFH histologically and reclassified 20 of the cases as leiomyosarcomas. Considering these findings together with recent DNA microarray and comparative genomic hybridization analyses [25, 31, 32], at least a proportion of MFHs should be reclassified as a pleomorphic subtype of leiomyosarcoma. In this context, pleomorphic leiomyosarcoma and MFH shared similar expression patterns of tropomyosin isoforms.

The similarity of the protein expression profiles of clear cell sarcoma, synovial sarcoma, and MPNST is consistent with the biologic associations and similar gene expression patterns of these tumors. Clear cell sarcoma is also known as melanoma of soft parts and is derived from neural crest progenitor cells [19]. Nagayama et al. [30] reported synovial sarcoma and MPNST shared similar expression patterns of numerous genes related to neural differentiation and suggested synovial sarcoma might be of neuroectodermal origin. On the basis of protein expression patterns, our present results appear to support the assumption that these three tumors are derived from (or differentiate to) neural or neuroectodermal cells.

Currently, the therapeutic strategy for bone and soft tissue sarcomas largely depends on the histologic subtype, grade, and stage of the disease [11, 26]. Although the systems provide valuable information about the clinical behavior of the tumors in most cases, there are several outliers (or patients) in which their clinical course could not be predicted only on the basis of classic appraisals. Moreover, the introduction of molecular-targeted drugs has changed the situation dramatically [8, 28, 41]. Most of these new drugs target a specific molecule, whose presence could not be predicted only from the classic clinicopathologic features. Novel clues for identifying prognostic markers and therapeutic targets in individual tumors are urgently required.

GISTs are the most common mesenchymal tumors of the gastrointestinal tract and are characterized by a wide spectrum of clinical outcomes [41]. Identification of a high-risk group of patients who may benefit from adjuvant therapy such as that including imatinib is an urgent clinical concern. We found 43 proteins, including eight variants of pfetin, which was originally reported as a protein highly expressed in fetal cochlea and brain, were correlated with the outcome of patients with GIST [35, 38]. Although the expression of a whole 43-protein set predicted the outcome of GIST correctly, it seemed difficult to apply the results directly to a hospital setting. Cutting-edge genome or proteome technologies cannot be transferred easily to ordinary clinical examinations. A smaller number of targets, measurable by simpler methods such as immunohistochemistry, is preferable for use in practice. We found expression of pfetin protein, which could be examined immunohistochemically using paraffin-embedded archival tissues, predicted ($p < 0.0001$) disease-specific survival in patients with GIST [38]. Examination of pfetin expression using immunohistochemistry may allow the identification of high-risk patients with GIST who may benefit from adjuvant treatment such as that including imatinib and minimize the risk of unnecessary treatment for low-risk patients.

The prognosis of patients with osteosarcoma has improved markedly as a result of effective chemotherapy. Dose-intensive multiagent chemotherapy continued for 1 year or so has resulted in long-term survival for the majority of patients with localized osteosarcoma [27]. Despite this success, however, 30% to 40% of patients, mainly those with tumors showing a poor response to preoperative chemotherapy, will experience relapse, most often with pulmonary metastases, and die [2]. Prediction of chemosensitivity at the time of diagnosis would therefore be of great clinical importance. Over the last decade, considerable efforts have been made for this purpose. Not only classic parameters such as histologic subtype, tumor location, and presence of metastatic disease at diagnosis [1], but also several molecules related to drug metabolism/transport or tumor development have been reported to correlate with the chemosensitivity of osteosarcoma [3, 15, 17, 23].

Based on the results of cDNA microarray consisting of 23,040 genes, Ochi et al. [34] identified 60 genes whose expression was likely correlated with the chemosensitivity of osteosarcoma and proposed a scoring system based on the expression levels of these genes. Comprehensive analysis of expression levels among thousands of genes enables investigators to identify novel important molecules

that cannot be predicted from conventional data. Mintz et al. [29] reported osteosarcoma chemoresistance was associated with osteoclastogenesis and bone resorption based on decreased expression of osteoclastogenesis-inhibitory factors in tumors showing a poor response to chemotherapy. We report here 10 protein spots associated with the chemosensitivity (necrosis rate) of osteosarcoma to preoperative chemotherapy. Although the 10 spots are currently under investigation, further studies may lead to new diagnostic or prognostic markers for osteosarcoma and new therapeutic targets.

Proteomic analysis using 2D-DIGE can provide important, novel clues for understanding the biology of bone and soft tissue sarcomas and for revealing candidate tumor markers and therapeutic targets.

Acknowledgments We thank Robert Nakayama, Eisuke Kobayashi, and Ako Hosono for helpful and stimulating discussions and Misuzu Mori for technical assistance.

References

1. Bacci G, Ferrari S, Delepine N, Bertoni F, Picci P, Mercuri M, Bacchini P, Brach del Prever A, Tienghi A, Camandone A, Campanacci M. Predictive factors of histologic response to primary chemotherapy in osteosarcoma of the extremity: study of 272 patients preoperatively treated with high-dose methotrexate, doxorubicin, and cisplatin. *J Clin Oncol.* 1998;16:658-663.
2. Bacci G, Longhi A, Fagioli F, Briccoli A, Versari M, Picci P. Adjuvant and neoadjuvant chemotherapy for osteosarcoma of the extremities: 27 year experience at Rizzoli Institute, Italy. *Eur J Cancer.* 2005;41:2836–2845.
3. Baldini N, Scotlandi K, Barbanti-Brodano G, Manara MC, Maurici D, Bacci G, Bertoni F, Picci P, Sottili S, Campanacci M, Serra M. Expression of p-glycoprotein in high-grade osteosarcoma in relation to clinical outcome. *N Engl J Med.* 1995;333: 1380–1385.
4. Chen G, Gharib TG, Huang CC, Taylor JMG, Misek DE, Kardia SLR, Giordano TJ, Iannettoni MD, Orringer MB, Hanash SM, Beer DG. Discordant protein and mRNA expression in lung adenocarcinomas. *Mol Cell Proteomics.* 2002;1:304–313.
5. Cormier JN, Pollock RE. Soft tissue sarcomas. *CA Cancer J Clin.* 2004;54:94–109.
6. de Alava E. Molecular pathology in sarcomas. *Clin Transl Oncol.* 2007;9:130–144.
7. Fletcher CDM, Gustafson P, Rydholm A, Willen H, Akerman M. Clinicopathologic re-evaluation of 100 malignant fibrous histiocytomas: prognostic relevance of subclassification. *J Clin Oncol.* 2001;19:3045–3050.
8. Goodman VL, Rock EP, Dagher R, Ramchandani RP, Abraham S, Gobburu JVS, Booth BP, Verbois SL, Morse DE, Liang CY, Chidambaram N, Jiang JX, Tang S, Mahjoob K, Justice R, Pazdur R. Approval summary: sunitinib for the treatment of imatinib refractory or intolerant gastrointestinal stromal tumors and advanced renal cell carcinoma. *Clin Cancer Res.* 2007;13: 1367–1373.
9. Grier HE, Krailo MD, Tarbell NJ, Link MP, Fryer CJH, Pritchard DJ, Gebhardt MC, Dickman PS, Perlman EJ, Meyers PA, Donaldson SS, Moore S, Rausen AR, Vietti TJ, Miser JS. Addition of ifosfamide and etoposide to standard chemotherapy for Ewing's sarcoma and primitive neuroectodermal tumor of bone. *N Engl J Med.* 2003;348:694–701.
10. Grimer RJ. Surgical options for children with osteosarcoma. *Lancet Oncol.* 2005;6:85–92.
11. Guillou L, Coindre JM, Bonichon F, Bui NB, Terrier P, Collin F, Vilain MO, Mandard AM, Doussal VL, Leroux A, Jacquemier J, Duplay H, Sastre-Garau X, Costa J. Comparative study of the National Cancer Institute and French Federation of Cancer Centers Sarcoma Group grading systems in a population of 410 adult patients with soft tissue sarcoma. *J Clin Oncol.* 1997;15: 350–362.
12. Gygi SP, Rochon Y, Franza BR, Aebersold R. Correlation between protein and mRNA abundance in yeast. *Mol Cell Biol.* 1999;19:1720–1730.
13. Hasegawa T, Hasegawa F, Hirose T, Sano T, Matsuno Y. Expression of smooth muscle markers in so called malignant fibrous histiocytomas. *J Clin Pathol.* 2003;56:666–671.
14. Holt GE, Schwartz HS, Caldwell RL. Proteomic profiling in musculoskeletal oncology by MALDI mass spectrometry. *Clin Orthop Relat Res.* 2006;450:105–110.
15. Ifergan I, Meller I, Issakov J, Assaraf YG. Reduced folate carrier protein expression in osteosarcoma: implications for the prediction of tumor chemosensitivity. *Cancer.* 2003;98:1958–1966.
16. Janknecht R. EWS-ETS oncoproteins: the linchpins of Ewing tumors. *Gene.* 2005;363:1–14.
17. Kakar S, Mihalov M, Chachlani NA, Ghosh L, Johnstone H. Correlation of c-fos, p53, and PCNA expression with treatment outcome in osteosarcoma. *J Surg Oncol.* 2000;73:125–126.
18. Kasper B, Lehnert T, Bernd L, Mechtersheimer G, Goldschmidt H, Ho AD, Egerer G. High-dose chemotherapy with autologous peripheral blood stem cell transplantation for bone and soft-tissue sarcomas. *Bone Marrow Transplant.* 2004;34:37–41.
19. Kawai A, Hosono A, Nakayama R, Matsumine A, Matsumoto S, Ueda T, Tsuchiya H, Beppu Y, Morioka H, Yabe H. Clear cell sarcoma of tendons and aponeuroses: a study of 75 patients. *Cancer.* 2007;109:109–116.
20. Kawai A, Muschler GF, Lane JM, Otis JC, Healey JH. Prosthetic knee replacement after resection of a malignant tumor of the distal part of the femur. *J Bone Joint Surg Am.* 1998;80:636–647.
21. Kondo T, Hirohashi S. Application of highly sensitive fluorescent dyes (CyDye DIGE Fluor saturation dyes) to laser microdissection and two-dimensional difference gel electrophoresis (2D-DIGE) for cancer proteomics. *Nat Protoc.* 2007;1:2940–2956.
22. Kondo T, Seike M, Mori Y, Fujii K, Yamada T, Hirohashi S. Application of sensitive fluorescent dyes in linkage of laser microdissection and two-dimensional gel electrophoresis as a cancer proteomic study tool. *Proteomics.* 2003;3:1758–1766.
23. Kusuzaki K, Takeshita H, Murata H, Hirata M, Hashiguchi S, Ashihara T, Hirasawa Y. Relation between cellular doxorubicin binding ability to nuclear DNA and histologic response to preoperative chemotherapy in patients with osteosarcoma. *Cancer.* 1998;82:2343–2349.
24. Ladanyi M. Fusions of the SYT and SSX genes in synovial sarcoma. *Oncogene.* 2001;5755–5762.
25. Lee YF, John M, Edwards S, Clark J, Flohr P, Maillard K, Edema M, Baker L, Mangham DC, Grimer R, Wooster R, Thomas JM, Fisher C, Judson I, Cooper CS. Molecular classification of synovial sarcomas, leiomyosarcomas and malignant fibrous histiocytomas by gene expression profiling. *Br J Cancer.* 2003;88: 510–515.
26. Mariani L, Miceli R, Kattan MW, Brennan MF, Colecchia M, Fiore M, Casali PG, Gronchi A. Validation and adaptation of a nomogram for predicting the survival of patients with extremity soft tissue sarcoma using a three-grade system. *Cancer.* 2005; 103:402–408.

27. Marina N, Gebhardt M, Teot L, Gorlick R. Biology and therapeutic advances for pediatric osteosarcoma. *The Oncologist.* 2004;9:422–441.
28. Milano A, Apice G, Ferrari E, Fazioli F, de Rosa V, de Luna AS, Iaffaioli RV, Caponigro F. New emerging drugs in soft tissue sarcoma. *Crit Rev Oncol Hematol.* 2006;59:74–84.
29. Mintz MB, Sowers R, Brown KM, Hilmer SC, Mazza B, Huvos AG, Meyers PA, LaFleur B, McDonough WS, Henry MM, Ramsey KE, Antonescu CR, Chen W, Healey JH, Daluski A, Berens ME, MacDonald TJ, Gorlick R, Stephan DA. An expression signature classifies chemotherapy-resistant pediatric osteosarcoma. *Cancer Res.* 2005;65:1748–1754.
30. Nagayama S, Katagiri T, Tsunoda T, Hosaka T, Nakashima Y, Araki N, Kusuzaki K, Nakayama T, Tsuboyama T, Nakamura T, Imamura M, Nakamura Y, Toguchida J. Genome-wide analysis of gene expression in synovial sarcomas using a cDNA microarray. *Cancer Res.* 2002;62:5859–5866.
31. Nakayama R, Nemoto T, Takahashi H, Ohta T, Kawai A, Seki K, Yoshida T, Toyama Y, Ichikawa H, Hasegawa T. Gene expression analysis of soft tissue sarcomas: characterization and reclassification of malignant fibrous histiocytoma. *Mod Pathol.* 2007;20:749–759.
32. Nielsen TO, West RB, Linn SC, Alter O, Knowling MA, O'Connell JX, Zhu S, Fero M, Sherlock G, Pollack JR, Brown PO, Botstein D, van de Rijn M. Molecular characterization of soft tissue tumours: a gene expression study. *Lancet.* 2002;359:1301–1307.
33. Oberlin O, Rey A, Desfachelles AS, Philip T, Plantaz D, Schmitt C, Plouvier E, Lejars O, Rubie H, Terrier P, Michon J. Impact of high-dose busulfan plus melphalan as consolidation in metastatic Ewing tumors. *J Clin Oncol.* 2006;24:3997–4002.
34. Ochi K, Daigo Y, Katagiri T, Nagayama S, Tsunoda T, Myoui A, Naka N, Araki N, Kudawara I, Ieguchi M, Toyama Y, Toguchida J, Yoshikawa H, Nakamura Y. Prediction of response to neoadjuvant chemotherapy for osteosarcoma by gene-expression profiles. *Int J Oncol.* 2004;24:647–655.
35. Resendes BL, Kuo SF, Robertson NG, Giersch ABS, Honrubia D, Ohara O, Adams JC, Morton CC. Isolation from cochlea of a novel human intronless gene with predominant fetal expression. *J Assoc Res Otolaryngol.* 2004;5:185–202.
36. Rosen G, Caparros B, Huvos AG, Kosloff C, Nirenberg A, Cacavio A, Marcove RC, Lane JM, Mehta B, Urban C. Preoperative chemotherapy for osteogenic sarcoma: selection of postoperative adjuvant chemotherapy based on the response of the primary tumor to preoperative chemotherapy. *Cancer.* 1982;15:1221–1230.
37. Suehara Y, Kondo T, Fujii K, Hasegawa T, Kawai A, Seki K, Beppu Y, Nishimura T, Kurosawa H, Hirohashi S. Proteomic signatures corresponding to histological classification and grading of soft-tissue sarcomas. *Proteomics.* 2006;6:4402–4409.
38. Suehara Y, Kondo T, Seki K, Shibata T, Fujii K, Goto M, Hasegawa T, Shimada Y, Sasako M, Shimoda T, Kurosawa H, Beppu Y, Kawai A, Hirohashi S. Pfetin, as a prognostic biomarker of gastrointestinal stromal tumors revealed by proteomics. *Clin Cancer Res.* 2008;14:1707–1717.
39. Tschoep K, Kohlmann A, Schlemmer M, Haferlach T, Issels RD. Gene expression profiling in sarcomas. *Crit Rev Oncol Hematol.* 2007;63:111–124.
40. Tunn PU, Schmidt-Peter P, Pomraenke D, Hohenberger P. Osteosarcoma in children: long-term functional analysis. *Clin Orthop Relat Res.* 2004;421:212–217.
41. Van der Zwan SM, DeMatteo RP. Gastrointestinal stromal tumor: 5 years later. *Cancer.* 2005;104:1781–1788.

VOLUME 26 · NUMBER 25 · SEPTEMBER 1 2008

JOURNAL OF CLINICAL ONCOLOGY

ORIGINAL REPORT

Distinct Gene Expression–Defined Classes of Gastrointestinal Stromal Tumor

Umio Yamaguchi, Robert Nakayama, Kazufumi Honda, Hitoshi Ichikawa, Tadashi Hasegawa, Miki Shitashige, Masaya Ono, Ayako Shoji, Tomohiro Sakuma, Hideya Kuwabara, Yasuhiro Shimada, Mitsuru Sasako, Tadakazu Shimoda, Akira Kawai, Setsuo Hirohashi, and Tesshi Yamada

From the Chemotherapy Division and Cancer Proteomics Project; Cancer Transcriptome Project, National Cancer Center Research Institute; Orthopaedic Surgery, Gastrointestinal Oncology, Gastric Surgery, and Clinical Laboratory Divisions, National Cancer Center Hospital; BioBusiness Group, Mitsui Knowledge Industry, Tokyo; and the Department of Surgical Pathology, Sapporo Medical University School of Medicine, Sapporo, Japan.

Submitted August 29, 2007; accepted May 14, 2008.

Supported by the Program for Promotion of Fundamental Studies in Health Sciences, conducted by the National Institute of Biomedical Innovation of Japan, the Third-Term Comprehensive Control Research for Cancer, conducted by the Ministry of Health, the Labor and Welfare of Japan and the Ministry of Education, Culture, Sports, Science and Technology of Japan, and generous grants from the Naito Foundation and the Princess Takamatsu Cancer Research Fund. U.Y. is an awardee of a Research Resident Fellowship from the Foundation for Promotion of Cancer Research (Tokyo, Japan). These fund resources played no role in designing and interpreting the results of this study.

Microarray data of this study have been submitted to the GEO (Gene Expression Omnibus) database (accession number GSE8167).

Terms in blue are defined in the glossary, found at the end of this article and online at www.jco.org.

Authors' disclosures of potential conflicts of interest and author contributions are found at the end of this article.

Corresponding author: Tesshi Yamada, MD, PhD, Chemotherapy Division and Cancer Proteomics Project, National Cancer Center Research Institute, 5-1-1 Tsukiji, Chuo-ku, Tokyo 104-0045, Japan; e-mail: tyamada@gan2.res.ncc.go.jp.

0732-183X/08/2625-4100/$20.00

DOI: 10.1200/JCO.2007.14.2331

ABSTRACT

Purpose
The majority of gastrointestinal stromal tumors (GIST) can be cured by surgery alone, but relapse occurs in 20% to 40% of cases. GISTs are considered to invariably arise through gain of function *KIT* or *PDGFA* mutation of the interstitial cells of Cajal (ICC). However, the genetic basis of the malignant progression of GISTs are poorly understood.

Patients and Methods
The expression levels of 54,613 probe sets in 32 surgical samples of untreated GISTs of the stomach and small intestine were analyzed with oligonucleotide microarrays. The representative GeneChip data were validated by real-time reverse transcriptase polymerase chain reaction and immunohistochemistry.

Results
Unbiased hierarchical clustering consistently separated the 32 cases of GIST into two major classes according to tumor site. The two major classes were further separated into novel subclasses, which were significantly correlated with various pathological prognostic parameters, the frequency of metastasis ($P < .05$), and clinical outcome. Immunohistochemical analysis of 152 independent patients with gastric GISTs revealed that the expression of dipeptidyl peptidase IV (T-cell activation antigen CD26) protein was significantly associated with poorer overall and disease-free survival ($P < .00001$).

Conclusion
CD26 appears to be a reliable biomarker of malignant GISTs of the stomach. The postoperative recurrence rate of CD26-negative cases was as low as 2.0% (two of 102). Therefore, postoperative follow-up of such patients might be made less intensive. CD26 may play an important role in the malignant progression of gastric GISTs and serve as a therapeutic target.

J Clin Oncol 26:4100-4108. © 2008 by American Society of Clinical Oncology

INTRODUCTION

Gastrointestinal stromal tumors (GISTs) are an established human tumor entity characterized by distinct clinical, genetic, and histopathological features.[1-3] The overall frequency of GISTs are estimated to be no more than 10 to 20 cases per million in Western countries,[1] but GISTs comprise the majority of primary mesenchymal tumors of the gastrointestinal tract. Approximately 60% to 70% of GISTs arise in the stomach, 20% to 30% in the small intestine, and 5% in the colon and rectum.[1,3] On the basis of similarities in immunohistochemical and ultrastructural features, it is considered that GISTs arise from interstitial cells of Cajal (ICC) or their precursor cells.[4] More than 80% of GISTs have gain of function mutations of the *KIT* proto-oncogene that encodes the c-Kit (CD117) receptor tyrosine kinase,[5] and one third of GISTs without *KIT* mutation carry reciprocal mutations in the *PDGFRA* gene that encodes platelet-derived growth factor receptor α (PDGFRA) tyrosine kinase.[6,7]

GISTs show a wide spectrum of clinical courses. The majority of cases can be cured by surgical resection alone, but 20% to 40% of cases relapse during the postsurgical follow-up.[8-10] Distant metastasis to the liver is the most common manifestation of recurrence,[10] and our previous experience indicates that the 5-year and 10-year survival rates after grossly curative surgery are 81.7% and 67.4%, respectively.[8] Many pathological criteria based on tumor site, size, cell type, degree of necrosis,[8,10-12] mitotic rate, Ki-67 immunoreactivity (MIB1 labeling) as well as their combinations have been proposed for predicting the outcome of patients with GISTs. The National Institutes of Health convened a

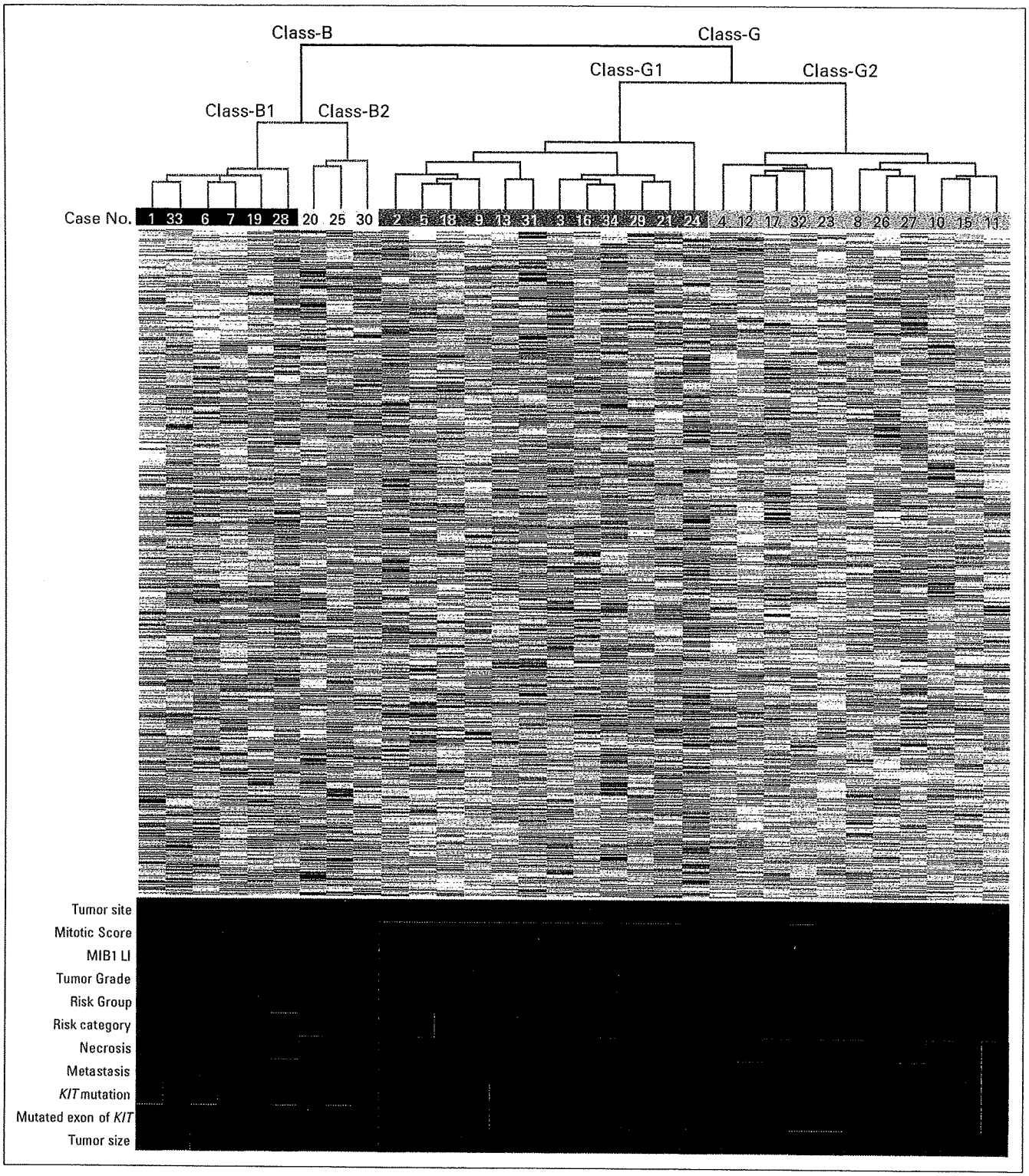

Fig 1. Four distinct gene expression–defined subclasses of gastrointestinal stromal tumors. Unsupervised hierarchical clustering separated 32 GIST cases into four subclasses based on the expression levels of the 21,214 probe sets of the GeneChip Human Genome U133 Plus 2.0 array (Affymetrix, Santa Clara, CA). Case numbers correspond to those of Appendix Table A1. The clinicopathological characteristics of the 32 cases in the four subclasses are indicated by red and green rows as follows: tumor site (red, small intestine/green, stomach), mitotic score (red, score 1/green, score 2), MIB1 labeling index (red, index 1/green index 2), tumor grade (red, grade 1/green, grade 2), risk group (red, low grade/green, high grade), risk category (red, low and intermediate risk/green, high risk), necrosis (red, absent/green, present), metastasis (red, absent/green, present), *KIT* mutation (red, absent/green, present), mutated exon of *KIT* (red, other than exon 11/green, exon 11), and tumor size (red, < 5 cm/green, ≥ 5.0 cm).

workshop in 2001, and a consensus (risk category) was proposed to estimate the relative risk of GISTs based on tumor size and mitotic count.[11] However, the cutoff values for these criteria have been determined empirically, and subjective assessments by skilled pathologists are inevitable. Therefore, it is necessary to identify an objective biomarker for recurrence of GISTs with a high positive or negative predictive value.

Imatinib mesylate (STI-571/Gleevec; Novartis Pharma, Basel, Switzerland), which selectively inhibits a group of tyrosine kinase receptors including *KIT* and *PDGFRA*, has been proven to be effective for the management of recurrent and unresectable GISTs.[13,14] However, the effect of imatinib mesylate varies depending on the domains of *KIT* and *PDGFRA* affected by the mutations.[15] Imatinib treatment is generally safe, but serious events such as gastrointestinal and intra-abdominal hemorrhage have been reported.[16,17] Furthermore, drug-refractory tumor cells develop due to second mutations of *KIT* during continuous therapy.[18] Although several clinical studies are currently underway to investigate the efficacy of emerging kinase inhibitors,[19,20] it is necessary to identify a new target molecule other than *KIT* or *PDGFR*.

In this study, we analyzed a well-characterized cohort of GIST cases in order to clarify the genomic alterations associated with the malignant progression of this tumor and to identify a biomarker that might be applicable to the prediction of outcome in patients with GISTs.

PATIENTS AND METHODS

Tumor Samples

All of the samples were obtained surgically at the National Cancer Center Hospital (Tokyo, Japan) between July 1972 and November 2005. Fresh frozen tumor specimens of 32 cases of GISTs of the stomach and small intestine were used for GeneChip (Affymetrix, Santa Clara, CA) analysis, and formalin-fixed paraffin-embedded tissue sections of 152 other cases of gastric GIST cases were used for independent validation. The study protocol for collection of tumor samples and clinical information was approved by the institutional review board, and patients provided written informed consent authorizing the collection and use of the tumor samples for research purposes.

Clinicopathological Assessment and Mutation Analysis

Immunohistochemistry for c-Kit, CD34, and Ki-67 was performed as described previously.[21,22] Mitotic score was determined by counting the number of mitotic figures in 10 consecutive high-power fields (HPF; ×400). Score 1 was ≤ 5 per 10 HPF, and score 2 was > 5 per 10 HPF. MIB1 labeling index (LI) was assigned as index 1 (< 10% MIB1-positive cells) and index 2 (≥ 10% MIB1-positive cells). Tumor grade was defined as grade 1 (index 1 and no tumor necrosis) and grade 2 (index 2 or tumor necrosis). Risk group was

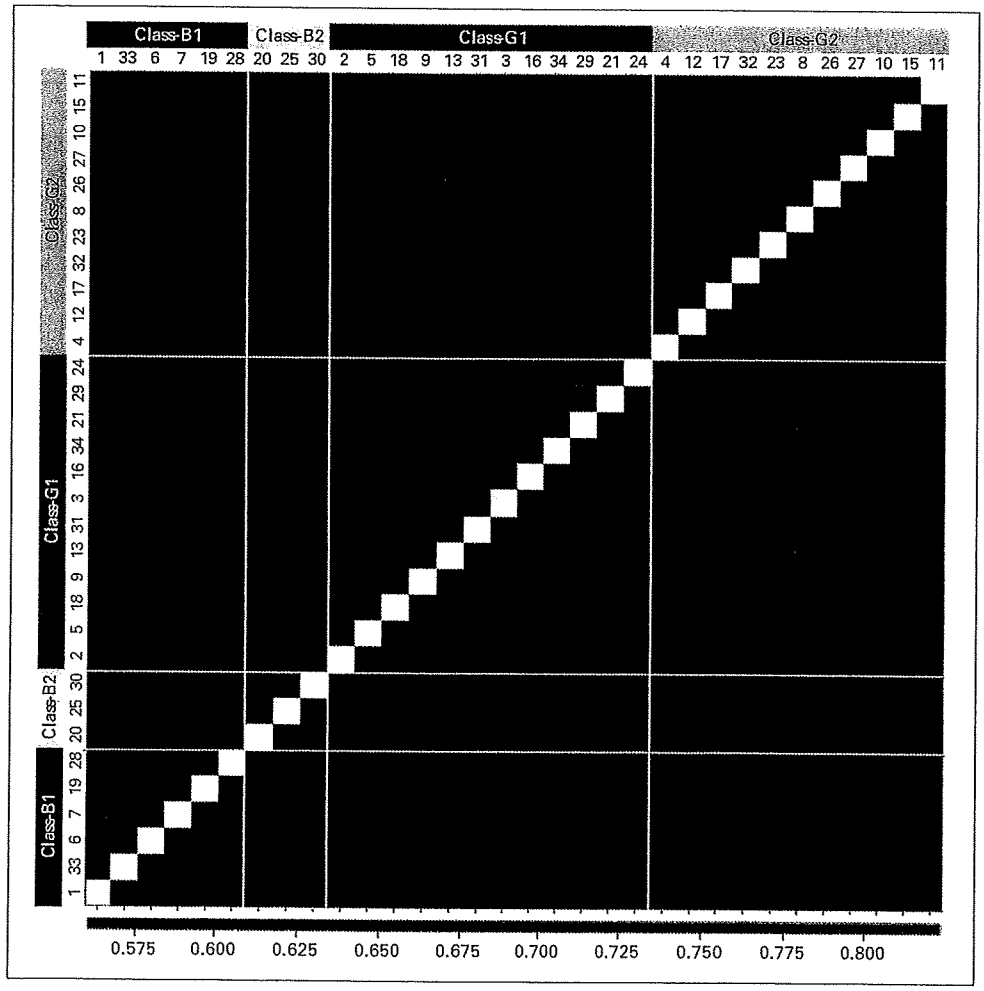

Fig 2. Heterogeneous gene expression of malignant gastrointestinal stromal tumors. The correlation coefficient value for each pair is shown in pseudo color according to the scale at the bottom. Red indicates higher correlation, and blue indicates lower correlation.

defined as low-risk group (grade 1 and tumor size of < 5.0 cm) and high-risk group (grade 1 and tumor size of ≥ 5.0 cm or any grade 2). Risk category was defined as described previously.[11] The mutational status of the *KIT* and *PDGFRA* genes was determined as described previously.[23]

GeneChip Analysis

Total RNA was extracted with IsoGen lysis buffer (Nippon Gene, Toyama, Japan) and purified with a RNeasy Mini kit (Qiagen, Hilden, Germany). We used GeneChip Human Genome U133 Plus 2.0 arrays (Affymetrix) to analyze the mRNA expression levels of 54,613 probe sets corresponding to more than 38,000 human UniGene Clusters in accordance with the manufacturer's protocols. The background correction, probe summarization, and normalization of all the GeneChip data were performed with the Microarray Analysis Suite 5 algorithm, and the processed values of all probe sets were then log-transformed for subsequent analyses, using the ArrayAssist 4.0 software package (Stratagene, La Jolla, CA).

Hierarchical clustering analysis was performed with centered values of the Pearson's correlation coefficient and Ward's linkage method. Clustering analysis was performed by biostatisticians (A.S., T.S., H.K.) who were blinded to the clinicopathological data.

Real-Time Reverse-Transcriptase Polymerase Chain Reaction

For cDNA synthesis, 5 μg of total RNA was reverse transcribed by random priming with Superscript II reverse transcriptase (Invitrogen). The gene-specific TaqMan primers and probes were designed by Applied Biosystems (Foster City, CA). Real-time reverse-transcriptase polymerase chain reaction (RT-PCR) was carried out using the ABI Prism 7000 Sequence Detection System (Applied Biosystems). The comparative C_t values were normalized to that of glyceraldehyde 3-phosphate dehydrogenase.[24]

Immunohistochemistry of CD26

Goat antihuman CD26 antibody (AF1180) was purchased from R&D Systems (Minneapolis, MN). Immunoperoxidase staining of formalin-fixed and paraffin-embedded tissue sections using the avidin-biotin complex was performed as described previously.[25] Immunohistochemical results were judged by three investigators (T.Y., K.H., U.Y.) without awareness of the clinical information. Endothelial cells of blood vessels served as internal positive controls. Tumors that showed any degree of CD26 staining were classified as positive.

Statistical Analysis

Estimates of overall and disease-free survival were computed using the Kaplan-Meier method using the StatFlex statistical software package version 5.0 (Artec, Osaka, Japan). Overall survival was calculated from the day of diagnosis until death or until the end of follow-up. Disease-free survival was calculated from the day of diagnosis until the day of relapse or death as a result of disease, whichever came first. Differences between survival curves were assessed for statistical significance with the log-rank test. Other statistical tests were performed using tools available in the R statistical package (version 2.0.1; http://www.r-project.org/).

RESULTS

Classification of GISTs Into Four Subclasses Based on Global Gene Expression

The clinicopathological, immunohistochemical, and genetic characteristics of the 32 cases of GIST used in the GeneChip analysis are presented in Appendix Table A1, online only.

To grasp the overall gene expression pattern, we first performed unsupervised analysis of all 54,613 probe sets. Hierarchical clustering separated the 32 GISTs into two principal classes, each of which was further divided into two subclasses (Appendix Fig A1, online only). To eliminate probes that had little or no variation across samples (probes that were not working well), we next selected a set of 21,214 probes showing intensity differences of more than 2^3-fold between the maximum and minimum signals across the 32 samples and repeated the same unsupervised analysis. Hierarchical clustering separated the 32 samples into the same four subclasses except for one sample (case 28; Fig 1). We further confirmed the stability of this gene expression–defined clustering by eliminating probe sets with intensity differences of less than 2^4-fold (6,231 probe sets), 2^5-fold (2,907 probe sets), and 2^6-fold (1,380 probe sets; data not shown).

Clinicopathological Significance of the Gene-Expression–Defined Subclasses

We named the two principal classes separated by unsupervised analysis of the 21,214 probe sets as class B (for bowel) and class G (for gastric), because all tumors of the small intestine were clustered into class B, and all tumors of the stomach were clustered into class G (Fig 1). The four subclasses were designated as class B1, class B2, class G1, and class G2 (from left to right in Fig 1). The subclasses were found to be associated with the known prognosis-relevant clinicopathogical variables (Fig 1). Fisher's exact test showed that there were significant differences between class B1 and class B2 as well as between class G1 and class G2 in the frequency of mitotic score, MIB1 LI, tumor grade, risk group, and metastasis ($P < .05$; Appendix Table A2, online only). There was no significant difference in the presence of *KIT* mutation, mutated exon of *KIT*, tumor size, cell type, sex, or expression of c-Kit or CD34 (Table A2 and data not shown). Mitotic score, MIB1 LI, tumor grade, risk group, and metastasis did not remain significantly different ($P < .05$) between class B1 and class B2, when Holm's adjustment of P values was applied for dealing with the multiple testing situation.[26]

Appendix Figure A2A and A2B shows the Kaplan-Meier plots for disease-free survival of patients in the subclasses. The gene expression–defined clusters clearly separated the patients into those with good outcome (class B1 and class G1) and those with poor outcome (class B2 and class G2; $P < .005$). Remarkably, none of the patients in class B1 or class G1 died during follow-up period of 108 months.

Heterogeneous Gene Expression of Malignant GISTs

The correlation coefficient values of 21,214 probe sets between all the combinations of the 32 GIST cases were calculated, and are presented as a pseudocolored heat map in Figure 2. There were high similarities of overall gene expression within cases of class B1 and

Table 1. Heterogeneous Gene Expression of Malignant Gastrointestinal Stromal Tumors

Class	No. of Pairs	Average Correlation Coefficient	CI	*t* Value	*df*	*P*
B1	15	0.78	0.77 to 0.79	5.72	3.11	.0096*
B2	3	0.69	0.64 to 0.74			
G1	66	0.74	0.73 to 0.75	3.69	95.93	.0004†
G2	55	0.71	0.71 to 0.72			

NOTE. Pearson's product-moment correlation coefficients were calculated among cases belonging to the same subclass, and were then Z-transformed to correct estimated errors to yield a normal distribution. The averages of these transformed values were compared between class B1 and class B2 as well as between class G1 and class G2 (Welch's *t*-test).
*< .01.
†< .001.

within cases of class G1, but not within cases of class B2 or within cases of class G2 (Fig 2). The average correlation coefficient values were significantly different between class B1 and class B2 ($P < .01$, Welch's t-test) as well as between class G1 and class G2 ($P < .001$; Table 1). These findings suggest that genomic diversity increases significantly during the malignant progression of GISTs.

Gene Expression Changes Associated With Malignant Progression of GISTs

There were 122 probe sets whose expression was increased in class B1 compared with class B2, and 400 probe sets whose expression was increased in class G1 compared with class G2 (Appendix Fig A3A, online only). There were 97 probe sets whose expression was increased in class B2 compared with class B1, and 321 probe sets whose expression was increased in class G2 compared with class G1 (Fig A3B). Only eight probe sets (eight UniGene clusters) were commonly increased in class B1 and class G1 relative to each respective counterpart (Fig A3A and Appendix Table A3), and 12 probe sets (12 UniGene clusters) were commonly increased in class B2 and class G2 relative to each respective counterpart (Fig A3B and Appendix Table A4), suggesting that the genomic alterations promoting malignant progression differ between small intestinal GISTs and gastric GISTs.

We conducted real-time RT-PCR analysis of 20 representative genes differentially expressed between class G1 and class G2 to validate the results of the GeneChip analysis. Appendix Figure A4 represents 10 of these 20 genes.

CD26 Is a Significant Prognostic Factor of Gastric GISTs

Among the 400 probe sets whose expression was significantly increased in class G2 compared with class G1, we noticed that the *DPP4* (dipeptidyl peptidase IV) gene (which encodes the CD26 protein) was ranked in the first, second, third, and fifth places (Appendix Table A8, online only). Immunohistochemistry of 21 gastric GIST cases for which specimens were available revealed there were 12 CD26-positive (Fig 3A, 3B, 3D, and 3E) and nine CD26-negative cases (Fig 3C and 3F). The expression of CD26 protein appeared to be correlated well with gene expression–defined classes except for one case (case 2; Fig 3G). The disease-free and overall survival of patients with CD26-positive GISTs was worse than that of patients with CD26-negative GISTs ($P < .05$; Appendix Fig A5, online only). Appendix

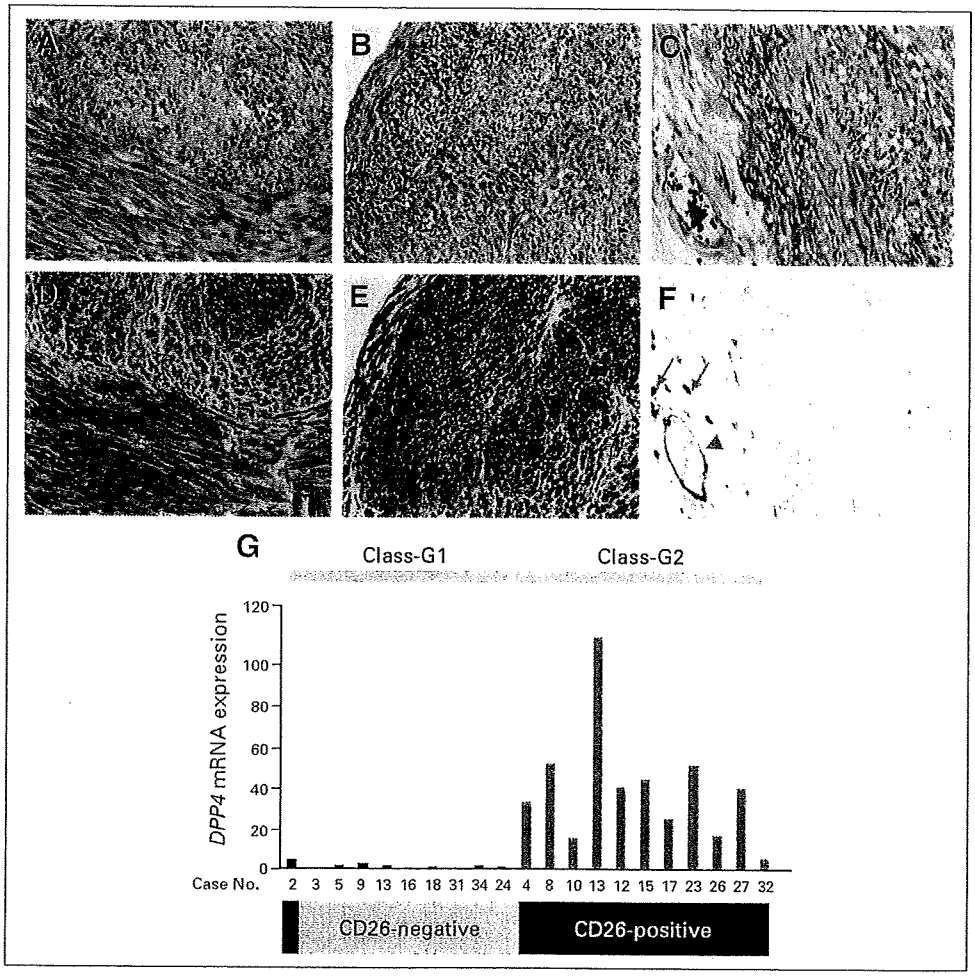

Fig 3. Correlation of dipeptidyl peptidase IV (*DPP4*) mRNA with CD26 protein expression. (A-C) Hematoxylin and eosin and (D-F) immunoperoxidase staining of (A, B, D, E) CD26-positive and (C, F) CD26-negative gastric gastrointestinal stromal tumors. The arrowhead indicates vascular endothelium, and arrows indicate CD26-positive inflammatory cells. (G) Relative *DPP4* mRNA expression level was determined by real-time reverse transcriptase polymerase chain reaction (in arbitrary units). The bar at the bottom indicates CD26-positive (black) and CD26-negative (gray) cases.

Table A5 (online only) presents the relationship between CD26 expression and gene expression–defined subclasses of small intestinal and gastric GISTs.

We then examined the clinical significance of CD26 protein expression in an independent validation cohort consisting of 152 gastric GISTs. The patients comprised 83 males (54.6%) and 69 females (45.4%). The average age at diagnosis was 59 years (range, 28 to 83 years), and the duration of follow-up ranged from 4 to 352 months (mean, 117 months). Follow-up computed tomography (CT) imaging was performed every 3 to 6 months. Of the 152 patients, 22 (14.5%) developed distant metastasis (14 to liver, four to peritoneum, two to bone, one to lung, and one to lymph node), seven of them were treated with imatinib mesylate. Immunohistochemically, 149 cases were positive for c-Kit, and 148 cases were positive for CD34.

Of the 152 gastric GISTs, 50 were CD26 positive (32.9%), and the remaining 102 were CD26 negative (67.1%). CD26 positivity was significantly ($P < .05$, Fisher's exact test) associated with tumor size, necrosis, mitotic score, MIB1 LI, tumor grade, risk group, risk category, and metastasis (Table 2). CD26 positivity was significantly associated with poor overall and disease-free survival ($P < .00001$; Fig 4A and 4B). The estimated overall survival rate at 10 years after surgery was 97.4% in CD26-negative patients and 69.9% in CD26-positive patients.

Table 2. Correlations Between Clinicopathological Characteristics and CD26 Expression in 152 Cases of Gastric Gastrointestinal Stromal Tumors

	CD26 Expression					
	Negative		Positive			
Characteristic	No.	%	No.	%	P^*	Holm's Method P
Tumor size, cm						
< 5.0	72	73.5	26	26.5	.0307	.0316
≥ 5.0	30	55.6	24	44.4		
Necrosis						
No	100	69.4	44	30.6	.0158	.0316
Yes	2	25.0	6	75.0		
Mitotic score						
1	101	79.5	26	20.5	4.46×10^{-13}	3.57×10^{-12}
2	1	4.0	24	96.0		
MIB1 labeling index						
Index 1	100	77.5	29	22.5	3.49×10^{-10}	2.44×10^{-9}
Index 2	2	8.7	21	91.3		
Tumor grade						
1	98	77.2	29	22.8	1.08×10^{-8}	5.38×10^{-8}
2	4	16.0	21	84.0		
Risk group						
Low grade	95	77.2	28	22.8	1.47×10^{-7}	5.88×10^{-7}
High grade	7	24.1	22	75.9		
Risk category						
Very low	8	100.0	0	0.0	2.99×10^{-6}	8.96×10^{-6}
Low	60	78.0	17	22.0		
Intermediate	25	64.1	14	35.9		
High	9	32.1	19	67.9		
Metastasis						
No	100	76.9	30	23.1	1.38×10^{-9}	8.31×10^{-9}
Yes	2	9.1	20	90.9		

NOTE. Differences at $P < .05$ were considered significant.
*Fisher's exact test.

Almost all the CD26-negative cases were MIB1 LI index 1 (100 of 102), but the CD26-positive cases comprised a mixture of index 1 (29 of 50) and index 2 (21 of 50; Table 2). MIB1 LI is known to represent cell proliferation activity. We hypothesized that the CD26-positive cases might be further stratified by MIB1 LI. As shown in Figures 4C and 4D, the 152 gastric GIST cases were divided into three groups: CD26 negative, CD26 positive and index 1, and CD26 positive and index 2. There were significant differences in disease-free survival among these three groups ($P < .01$).

DISCUSSION

Several microarray analyses using smaller numbers of GIST cases had been conducted before this study.[27-31] GISTs show gene expression profiles different from those of other mesenchymal tumors.[27,31] The status of *KIT*/*PDGFRA* mutation has been reported to affect the global gene expression profile of GISTs.[29,30] However, none of these studies investigated the clinicopathological significance of the gene expression profiles, probably because long-term follow-up (for 5 to 10 years or more) is necessary for assessing the clinical outcome of this generally low-grade malignant tumor.[10]

Unsupervised hierarchical clustering is a well-established statistical method that separates cases based on similarities and dissimilarities of overall gene expression.[32] GISTs are considered to invariably arise through gain of function *KIT* or *PDGFRA* mutation of ICC. Most GISTs are composed of a fairly uniform population of spindle cells.[3,11] Allander et al[27] reported marked homogeneity in the gene expression of GISTs with *KIT* mutation. We assumed that low-grade GISTs constitute a uniform population and could be separated from high-grade GISTs by simple unsupervised clustering. The most principal determinant that separated the 32 GIST cases in this study was the site of tumor origin: the small intestine (class B) or stomach (class G; Fig 1), similarly to findings reported previously.[29] The second most principle determinant, however, was exactly as anticipated. Low-grade GISTs constituted a population with homogeneous gene expression profiles (classes B1 and G1; Fig 2) and was separated from high-grade GISTs, which constituted a heterogeneous population (classes B2 and G2, Fig 2).

In order to apply the observations obtained using GeneChip analysis to clinical practice, we selected the *DPP4* gene, because its expression showed the greatest significant differences between class G1 and class G2. We further validated the clinical significance of the *DPP4* gene product, CD26, in a large independent cohort of gastric GIST cases (Fig 4 and Table 2). Because the postoperative recurrence rate of CD26-negative cases was as low as 2.0% (two of 102) even in this cohort, the postoperative follow-up of these patients could have been significantly less intensive. Objective assessment of CD26 expression is possible using formalin-fixed paraffin-embedded tissue specimens (Figs 3D to 3F) and can be readily incorporated into routine pathological diagnosis along with c-Kit and CD34. For these reasons, CD26 is considered to be a biomarker superior to other known prognostic parameters.

CD26 is not only a biomarker of malignant GISTs, but may also play an important role in malignant progression. CD26 is a 110-kDa cell membrane glycoprotein that belongs to the serine protease family (EC 3.4.14.5).[33] It is expressed on a wide variety of cell lineages including T lymphocytes, endothelial and epithelial

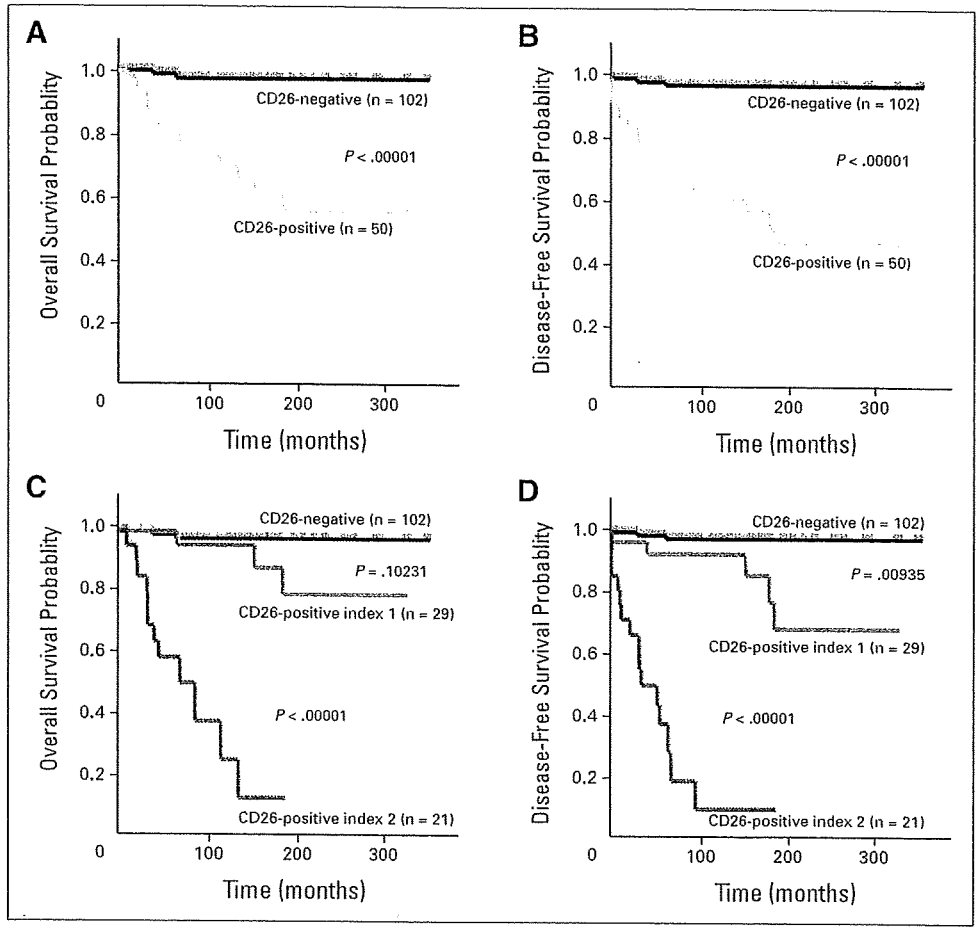

Fig 4. Correlation of CD26 expression with patient outcome in a validation cohort. (A) Kaplan-Meier analysis of overall survival of patients with CD26-positive (yellow) and CD26-negative (blue) gastric gastrointestinal stromal tumors (GISTs). (B) Kaplan-Meier analysis of disease-free survival of patients with CD26-positive (yellow) and CD26-negative (blue) gastric GIST. (C) Kaplan-Meier analysis of overall survival of patients with CD26-negative (blue), CD-26 positive and index 1 (gray), and CD-26 positive and index 2 (red) gastric GIST. (D) Kaplan-Meier analysis of disease-free survival of patients with CD26-negative (blue), CD-26 positive and index 1 (gray), and CD-26 positive and index 2 (red) gastric GIST.

cells. CD26 selectively cleaves the *N*-terminal dipeptide from cytokines and chemokines, and modulates their function. Although the role of CD26 in tumor development is still controversial,[33] an intriguing observation has been reported in a series of publications by Kotani and colleagues.[34,35] Differential diagnosis of follicular carcinoma of the thyroid from follicular adenoma has been one of the most difficult tasks for surgical pathologists. CD26 expression is highly specific to carcinoma and is able to predict distant metastasis of apparently benign thyroid tumors.[35] Unfortunately, CD26 expression was not associated with the outcome of small intestinal GISTs (data not shown), indicating that the molecular mechanisms behind the malignant progression of small intestinal GISTs differ from those of gastric GISTs. Further studies using cell culture and animal models are required to determine the exact biologic consequences of CD26 in GIST cells.

CD26 may serve as a therapeutic target molecule. Anti-CD26 monoclonal antibody has been shown to inhibit the growth of anaplastic large cell T-cell lymphoma both in vitro and in vivo.[36] Several orally active CD26 enzyme inhibitors have been developed as a new class of antidiabetic drugs. These inhibitors are generally safe and well tolerated, and no serious adverse effect has been noticed even in elderly patients.[37,38] These characteristics of CD26 inhibitors may make them suitable for long-term preventive administration to postoperative patients with GISTs.

At present, the precise molecular mechanism that induces the expression of CD26 remains to be clarified. CD26 may not be the cause of malignant progression of gastric GISTs, but its clear-cut association with the increased risk of postoperative recurrence warrants diagnostic application. It will certainly be necessary to validate our results in an independent study.

AUTHORS' DISCLOSURES OF POTENTIAL CONFLICTS OF INTEREST

The author(s) indicated no potential conflicts of interest.

AUTHOR CONTRIBUTIONS

Conception and design: Kazufumi Honda, Miki Shitashige, Masaya Ono, Tesshi Yamada
Financial support: Tesshi Yamada
Administrative support: Akira Kawai, Setsuo Hirohashi, Tesshi Yamada
Provision of study materials or patients: Tadashi Hasegawa, Yasuhiro Shimada, Mitsuru Sasako, Tadakazu Shimoda
Collection and assembly of data: Umio Yamaguchi, Robert Nakayama, Hitoshi Ichikawa, Tadashi Hasegawa
Data analysis and interpretation: Umio Yamaguchi, Kazufumi Honda, Miki Shitashige, Masaya Ono, Ayako Shoji, Tomohiro Sakuma, Hideya Kuwabara, Tesshi Yamada
Manuscript writing: Umio Yamaguchi, Tesshi Yamada
Final approval of manuscript: Tesshi Yamada

